Exploring the mechanism of biocatalyst inhibition in microbial desulfurization

Andres Abin-Fuentes[1], Magdy El-Said Mohamed[2], Daniel IC Wang[1] and Kristala LJ Prather[1*]

[1]Department of Chemical Engineering, Massachusetts Institute of Technology, Cambridge, MA, 02139, USA

[2]R&DC, Saudi Aramco, Dhahran 31311, Saudi Arabia

*author to whom correspondence should be directed

T: 617-253-1950, e-mail: kljp@mit.edu

Abstract

Microbial desulfurization or biodesulfurization (BDS) of fuels is a promising technology because it can desulfurize compounds that are recalcitrant to the current standard technology in the oil industry. One of the obstacles to the commercialization of BDS is the reduction in biocatalyst activity concomitant with the accumulation of the end product 2-hydroxybiphenyl (HBP) during the process. BDS experiments were performed by incubating *Rhodococcus erythropolis* IGTS8 resting cell suspensions with hexadecane at 0.50 vol/vol containing 10 mM dibenzothiophene. The resin Dowex® Optipore SD-2 was added to the BDS experiments at resin concentrations of 0, 10 or 50 g-resin/L-total. The HBP concentration within the cytoplasm was estimated to decrease from 1100 to 260 μM with increasing resin concentration. Despite this finding, productivity did not increase with resin concentration. This led us to focus on the susceptibility of the desulfurization enzymes towards HBP. Dose-response experiments were performed to identify major inhibitory interactions in the most common BDS pathway, the 4S pathway. HBP was responsible for three of the four major inhibitory interactions identified. The concentrations of HBP that led to 50% reduction in the enzymes' activities (IC_{50}) for DszA, DszB and DszC were measured to be 60 ± 5 μM, 110 ± 10 μM and 50 ± 5 μM, respectively. The fact that the IC_{50} values for HBP are all significantly smaller than the cytoplasmic HBP concentration suggests that the inhibition of the desulfurization enzymes by HBP is responsible for the observed reduction in biocatalyst activity concomitant with HBP generation.

Keywords: Enzyme inhibition, *Rhodococcus erythropolis* IGTS8, biodesulfurization, dibenzothiophene, 2-hydroxybiphenyl

Introduction

Biodesulfurization (BDS) is a process in which microorganisms, typically bacteria, are used to reduce the level of sulfur in fuels derived from crude oil including diesel and gasoline. BDS has gained interest over the last 20 years as an alternative to hydrodesulfurization (HDS), which is the current desulfurization standard in the oil industry. HDS uses a metal catalyst along with hydrogen gas (H_2) at high temperature and pressure to remove sulfur from organic sulfur compounds and generate H_2S gas (1). Major drawbacks of HDS include steric hindrance of the metal catalysts by certain recalcitrant compounds and large energy consumption due to process operation at high temperature and pressure (1). Recalcitrant compounds include the parent molecule dibenzothiophene (DBT) and some of its alkylated derivatives, such as 4-methyldibenzothiophene (4-DBT) and 4,6-dimethyldibenzothiophene (4,6-DBT). BDS can potentially be used to remove the sulfur that cannot be removed by HDS, though it is likely not a replacement for the current HDS infrastructure. The use of more than one desulfurization technology may be necessary to meet the increasingly stringent sulfur regulations (1).

There is a wide range of microorganisms known to have BDS capability (2). Such microorganisms typically desulfurize DBT by one of two pathways: the Kodama pathway or the 4S pathway (1). The Kodama pathway is a destructive BDS pathway in which carbon-carbon bonds in the DBT molecule are broken and sulfur is not selectively removed from the organic molecule. Due to its destructive nature, the Kodama pathway reduces the caloric value of the fuel that is being desulfurized. As a result, the majority of the focus on the past 20 years has been on the 4S pathway, which is an oxidative desulfurization pathway that cleaves the carbon-sulfur bond in DBT and leaves the carbon structure intact. The 4S pathway is a four-step enzymatic pathway that converts DBT to 2-hydroxybiphenyl (HBP) and sulfate (Figure 1). The

59 first two steps are the conversion of DBT to DBT-sulfoxide (DBTO) and then to DBT-sulfone
60 ($DBTO_2$). These steps are catalyzed by the enzymes DszC monooxygenase and DszD
61 oxidoreductase in synchrony. The third step is the conversion of $DBTO_2$ to 2-(2′-hydroxyphenyl)
62 benzene sulfinate (HBPS), which is catalyzed by DszA monooxygenase and DszD
63 oxidoreductase in synchrony. The final step is the conversion of HBPS to HBP and sulfite by
64 DszB desulfinase (3).
65 The isolation and purification of the desulfurization enzymes from *R. erythropolis* IGTS8
66 has been reported (4, 5). Preliminary characterization of these enzymes showed that DszB
67 catalyzes the slowest reaction with a turnover number (k_{cat}) of "about 2 min^{-1}" (4). Furthermore,
68 it was reported that DszA "has a turnover number (k_{cat}) of about 1/sec" (4). Following the
69 finding that DszB catalyzes the slowest step, the kinetics of DszB was investigated in detail (6).
70 DszB kinetics was modeled appropriately by the Michaelis-Menten model with a Michaelis
71 constant (K_m) of 0.90 ± 0.15 μM and a k_{cat} of 1.3 ± 0.07 min^{-1} (6). The kinetics of DszA, DszC,
72 and DszD from *R. erythropolis* IGTS8 have yet to be investigated in detail.
73 Two major obstacles facing BDS commercialization are that: (1) biocatalyst activities are
74 significantly lower than what is needed for BDS rates to match HDS rates (2); and (2)
75 biocatalysts cannot maintain activity for a long period of time. Considerable effort has gone into
76 trying to understand and overcome the limitations to the desulfurization activity of the
77 biocatalysts. Several studies have shown that genetic engineering can lead to higher
78 desulfurization activities (2). For example, the desulfurization activity of *R. erythropolis* KA2-5-
79 1 was increased from 50 to 250 μmol DBT/g DCW/h by providing multiple copies of the
80 desulfurization genes and placing them under the control of alternative promoters (2).
81 Reduction in biocatalyst activity over time has been widely reported in BDS processes (2,

7, 8). The reduction in activity is typically correlated to the accumulation of HBP in the medium during the BDS process. The desulfurization activity of a cell suspension of *R. erythropolis* IGTS8 of cell density 66 g DCW/L mixed with hexadecane (at 1:1 v/v ratio) containing 19000 μM DBT was found to follow first order decay with decay constant of 0.072 h^{-1} (7). It was suggested that the loss of biocatalyst activity might be due to exposure to increasing HBP concentrations, although no experiments were done to validate this hypothesis (7). The cells were active for 24 hours and only 7000 out of 19000 μM DBT in oil was consumed. The final concentration of HBP accumulated in the oil phase after 24 hours was only 3300 μM. Although aqueous phase accumulation of DBT or HBP was not measured, the contribution from the aqueous phase concentration to the overall concentration of either compound could not have been more than 5%. This was estimated based on the partition coefficients of DBT and HBP between hexadecane and water ($P_{O/W}$), which are 21000 and around 30-50, respectively (9). As a result, approximately 3600-3700 μM of DBT or HBP are unaccounted for at the end of the BDS process. Possible reasons for the discrepancy between DBT disappearance and HBP accumulation are accumulation of pathway intermediates or retention of DBT and/or HBP within the biocatalyst. *R. erythropolis,* being a gram-positive bacteria, has a cytoplasmic membrane surrounded by a thick cell wall made mostly of peptidoglycan. The cell wall is composed of thick peptidoglycan structure to which fatty acid molecules are attached. In the case of *R. erythropolis* (a member of the actinomycetes family), the cell wall is composed of mycolic acids that are perpendicular to the cell surface (10). These mycolic acids range from 30 to 54 carbon atoms in length and they make the cell wall of *R. erythropolis* highly hydrophobic. It is possible that a significant concentration of DBT initially in the oil phase would have been retained within the cell wall of *R. erythropolis* IGTS8 as it entered the cell. It is also possible that a significant

fraction of HBP produced by the biocatalyst would have been trapped within the biocatalyst cytoplasmic membrane or cell wall as it exited the cell. The amount of DBT or HBP retained by the biocatalyst will depend on the partition coefficients between the biocatalyst and the oil or aqueous phases, $P_{C/O}$ or $P_{C/W}$, respectively.

A number of studies have investigated the effect of HBP on biocatalyst activity. HBP has been shown to inhibit the growth of *R. erythropolis* IGTS8 at concentrations greater than 200 μM (11). Preliminary characterization of the DszB enzyme from *R.erythropolis* KA2-5-1 showed that its activity is reduced by 50% at HBP concentrations around 2000 μM (12). In other studies, the effect of exogenously added HBP on the BDS process has been described. *R. erythropolis* IGTS8 aqueous resting cell suspensions of 2 g DCW/L were prepared and supplied with only one of the 4S pathway compounds (either DBT, DBTO, $DBTO_2$ or HBPS) (13). HBP was also added at concentrations of either 0 and 50 μM in each experiment. The disappearance rate of each compound was monitored over a short period of 15 min. It was found that the disappearance rates of DBTO and HBPS were significantly reduced by the presence of 50 μM HBP. These results suggested that HBP might be inhibitory to the enzymes responsible for DBTO and HBPS consumption, which are DszC and DszB, respectively (Figure 1). In a different study, the DBT desulfurization rate of resting cells of *Microbacterium* sp. ZD-M2 was found to decrease significantly when HBP was added exogenously at concentrations ranging from 0-2000 μM (14). Results from experiments where HBP is added exogenously cannot be used to quantitatively predict the effect of HBP on a typical BDS process where DBT is added exogenously and HBP is generated endogenously within the cytoplasm of the cells. When HBP is added exogenously, a significant fraction may be retained by the cell wall and may never reach the cytoplasm, where inhibition of the desulfurization enzymes could occur. On the other hand,

HBP generated endogenously within the cytoplasm is immediately at the location where it can be inhibitory to the desulfurization enzymes. Therefore, the specific HBP loading of the biocatalyst (mg HBP/g DCW) that leads to a certain level of reduction in BDS activity may be significantly larger when HBP is added exogenously.

In summary, there is sufficient evidence to suggest that HBP (either generated endogenously or supplied exogenously) reduces the overall biocatalyst activity. In this work, a series of commercially available adsorbents were screened for their affinity and selectivity to adsorb HBP. The best adsorbent was used to determine whether or not HBP selective adsorbents could help mitigate the loss of desulfurization activity correlated with HBP accumulation during the BDS process. The kinetics and inhibition of the four enzymes in the 4S pathway by the intermediate compounds were next investigated in detail, in an attempt to understand the mechanism for the reduction in biocatalyst activity that is correlated with HBP accumulation.

Materials and Methods

Bacterial strains, vectors, media and chemicals. The DBT-desulfurizing strain used in this study was *Rhodococcus erythropolis* IGTS8 ATCC® 53968™, purchased from the American Type Culture Collection (USA). The defined minimal medium (MM) for cultivation contained (per liter of deionized water): glucose 30.0 g, NH_4Cl 3.0 g, $K_2HPO_4.3H_2O$ 6.75 g, $NaH_2PO_4.H_2O$ 2.25 g, $MgCl_2$ 0.245 g, $FeCl_3$ 4 mg, $CaCl_2$ 4 mg, Na_2SO_4 0.14 g, $ZnCl_2$ 32 mg, $MnCl_2.4H_2O$ 1 mg, $CuCl_2.2H_2O$ 5 mg, $Co(NO_3)_2.6H_2O$ 0.7 mg, $Na_2B_4O_7.10H_2O$ 0.7 mg, $(NH_4)_6Mo_7O_{24}.4H_2O$ 1 mg, EDTA 12 mg. Cryogenic stocks were prepared by addition of 15% (vol./vol.) glycerol (final concentration) to mid-log growth phase cultures in MM, which were then kept at -80°C for long term storage. Medium components were obtained from VWR International (USA). Dr.

Christine Nguyen, from Professor Stephen Buchwald's research group at MIT, kindly provided HBPS. All other chemicals were obtained from Sigma-Aldrich (USA). The strains used for expression of the desulfurization genes were *Escherichia coli* MAX Efficiency® DH10B™ and *E. coli* BL21 Star™ (DE3) One Shot® from Invitrogen™. The vector used for all molecular manipulations was pETDuet-1 from Novagen®. The medium used to culture these strains was Luria-Bertani (LB) broth from DIFCO® supplemented with ampicillin (100 μg/ml working concentration) for selection of clones containing the pETDuet-1 vector.

Testing HBP adsorbents. Activated charcoal, molecular sieves (of 4, 5, and 13 Å pores), Diaion® HP-20, Dowex® Optipore L-493, SD-2, Biobeads, Amberlite® XAD4, IRC86, IRA958 were all obtained from Sigma-Aldrich (USA). Resins were tested for their ability to adsorb HBP from a hexadecane-water solution. The adsorption experiments were carried out in 20 mL scintillation vials by mixing 5 mL of water with 5 mL of a hexadecane solution containing 10000 μM DBT and 10000 μM HBP with either 0.1 or 1.0 g of resin. Mixtures were equilibrated for 24 h at 30°C, with agitation at 250 rpm. After measuring solute concentrations before and after sample equilibration with a particular resin concentration (X_r), specific loadings (L_r) were determined by the following relationships:

$$X_r = \frac{m_r}{V_{total}} \tag{1}$$

$$L_r = \frac{\left(C_{HBP}\big|_{t_0} - C_{HBP}\big|_{t_{eq}}\right) MW_{HBP}}{X_r}, \tag{2}$$

where C_{HBP} represents the total concentration of HBP (in oil and water), V_{total} is the total volume of solution (oil plus water), m_r is the mass of resin used, X_r is the concentration of resin

172 employed, MW_{HBP} is the molecular weight of HBP (170 g/mole), and t_0 and t_{eq} represent time at
173 initial and equilibrium conditions, respectively.
174
175 *Resting cells preparation*. *R. erythropolis* IGTS8 cultures were grown in 400 mL of MM in a 2L
176 shake flask for a period of 40-48 hours during which the cell density increased from
177 approximately 0.03 g DCW/L to 3 g DCW/L. Cultures were centrifuged at 5000 RPM and 4°C
178 for 15 min and spent media was discarded. Biocatalyst pellets were resuspended to the
179 experimental cell density in 5 g/L glucose and 20 mM phosphate buffer pH 7.0.
180
181 *Four-component biodesulfurization experiments*. BDS experiments in the presence of Dowex®
182 Optipore SD-2 resin were carried out in 250 mL shake flasks containing 20 mL of a 15.5 g
183 DCW/L resting cell suspension mixed with 20 mL of hexadecane containing 10000 μM DBT.
184 The resin was added to the mixture at resin concentrations of X_r = 0, 10 or 50 g/L in the shake
185 flask and the flasks were incubated at 30°C for 26 hours. After the 26-hour incubation period,
186 the mixtures were centrifuged for 15 min at 5000 RPM and the four components (oil, water, cells
187 and resin) were separated. DBT and HBP concentrations in the oil and aqueous components
188 were measured directly after centrifugation. DBT and HBP concentrations in the cells and resin
189 were measured by extraction into ethanol. Ethanol was selected as the best extractant among a
190 variety of solvents tested, including acetone, methanol, hexane, hexadecane, squalane, and
191 toluene. Cell wall solubilization by treatment with an enzymatic mixture of lysozyme (100
192 mg/mL) and mutanolysin (5000 Units/mL) did not increase the concentration of DBT or HBP
193 extracted from the cells. Sonication of the cells also did not increase extraction concentrations.
194 Loadings of HBP on the biocatalyst (L_c) and resin (L_r) were calculated from the expressions:

$$L_c = \frac{\left(\sum_i C_{extract,i}\right) V_{extract}}{m_{cells}} \quad (3)$$

$$L_r = \frac{\left(\sum_i C_{extract,i}\right) V_{extract}}{m_{\text{resin}}}, \quad (4)$$

where $C_{extract,i}$ is the concentration of HBP in the *ith* extract, $V_{extract}$ is the volume of the extract (constant for each fraction), m_{cells} is the mass of cells extracted, and m_{resin} is the mass of resin extracted.

DNA manipulations and preparation of E. coli recombinant strains. Molecular biology manipulations were performed according to standard protocols. Genomic DNA was extracted from *R. erythropolis* IGTS8 using Promega's Wizard® genomic DNA purification kit. Each of the desulfurization genes was PCR-amplified from the extracted genomic DNA with appropriate primers (see Supplemental Material). Restriction sites for EcoRI and HindIII were included in the primers. PCR amplicons were then cut with the appropriate restriction enzymes and ligated with the pET-Duet vector that had been previously cut with the corresponding restriction enzymes. The resulting vectors containing the four genes (*dszA, dszB, dszC* and *dszD*) were sequence-verified. Each of the 4 vectors was then used to transform *E. coli* DH10B by electroporation using 1 mm pathlength cuvettes. *E. coli* BL21 Star™ (DE3) One Shot® was used as the expression host for each of the four desulfurization proteins, and transformed according to the manufacturer's protocol (Invitrogen). Ampicillin selection (100 μg/mL) was used to identify successful transformants.

Protein expression and purification protocol. The following protocol was followed to express and purify each of the four desulfurization enzymes:

1. A transformed *E. coli* BL21 colony from an LB-ampicillin plate was picked and grown in 10 mL LB with ampicillin at 30°C overnight.
2. The next day, 1 L of LB medium with ampicillin was inoculated with 10 mL of overnight culture and grown at 30°C with shaking at 250 RPM.
3. The 1L culture was induced with 0.3 mM IPTG when the OD_{600} of the culture was 0.5-0.6. Growth was continued for 18 hours at 20°C.
4. Cells were harvested by centrifugation at 5000 RPM for 15 minutes at 4°C.
5. The supernatant was discarded and the cell pellet was frozen at -20°C overnight.
6. From this point on all cells and protein samples were maintained at 4°C or on ice to avoid protein degradation. The cell pellet was resuspended using a volume of the 1X His buffer (with 10% glycerol) equal to at least 2.5 times the mass of the cell pellet. Lysozyme (1 mg/mL) and DNAseI (500 μg/mL) were added and the cell suspension was incubated for 30 minutes on ice.
7. The cell suspension was sonicated for 15-30 minutes at 90-100% amplitude with 1-second on/1-second off cycle.
8. Cell debris was pelleted by centrifugation at 20,000 rpm for 30 minutes at 4°C.
9. The supernatant (20-40 mL) was mixed with 5 mL Ni-NTA agarose (Qiagen) in order to bind the histidine-tagged desulfurization protein to the resin. The time for this binding step was 1 hour at 4°C.

10. After the 1 hour binding step, the protein-resin mixture was poured onto a Pierce® centrifuge column (10 mL total volume) and the resin was allowed to settle. The flow-through was processed by gravity flow and collected.

11. The resin was washed with 10 mL of 1X His buffer containing 7.5 mM imidazole and the flow through was collected. Then, the resin was treated with five different solutions of 1X His buffer containing increasing imidazole concentrations of: 40, 60, 100, 250 and 500 mM imidazole. Each solution was 5 mL in volume. The eluent of each fraction was collected.

12. A diagnostic SDS-PAGE gel was run to determine the fractions with the highest purity. These fractions were combined in one piece of snakeskin dialysis tubing and the protein sample was dialyzed overnight in 1L of 50 mM Tris-HCl/50 mM NaCl/10% glycerol buffer in the cold room with mild stirring.

13. Finally, the dialyzed protein was flash-frozen using liquid nitrogen in small aliquots for long-term storage at -80°C.

Enzyme assays.

All enzyme assays were performed in 20 mM phosphate buffer at pH 7.0 and 30°C. The assay volume was 1000 μL for all assays. DszD assays were performed in semi-micro cuvettes and maintained at room temperature. DszA, DszB and DszC assays were performed in 1.7 mL Eppendorf tubes in a rotary shaker incubator at 30°C and 250 RPM and were quenched either by addition of 1% of a 12 M HCl solution or by using an Amicon Ultra-0.5 mL 10 kDa spin filter device to remove the enzyme. For DszD enzyme assays, either the concentration of NADH was varied from 0-400 μM (at fixed FMN = 100 μM) or the concentration of FMN was varied from

0-100 μM (at fixed NADH = 150 μM), the concentration of DszD enzyme was 1.2 μg/mL, and the assays were run for 10 minutes. For DszC enzyme assays, the concentration of NADH was 500 μM, FMN concentration was 10 μM, DBT concentration was varied from 0-5 μM, DszD concentration was 0.47 μg/mL, DszC concentration was 3.1 μg/mL and the assays were run for 5 minutes. Assay conditions were identical for determining the mechanism of DszC inhibition by HBPS and HBP except for the addition of those compounds at concentrations of 0-200 and 0-1000 μM, respectively. For DszA enzyme assays, the NADH concentration was 500 μM, FMN concentration was 10 μM, $DBTO_2$ was varied from 0-80 μM, DszD concentration was 1.4 μg/mL, DszA concentration was 6.7 μg/mL, and the assays were run for 3 min. For DszB enzyme assays, the HBPS concentration was varied from 0-200 μM, DszB concentration was 3.5 μg/mL, and the assays were run for 5 min. For all four enzymes dose-response type assays were performed to measure the inhibitory concentration leading to 50% reduction in enzyme activity (IC_{50}). For DszD dose-response assays, the concentration of NADH was 500 μM and that of FMN was 200 μM, the concentration of the various pathway intermediates was varied (DBT: 0-5 μM, $DBTO_2$: 0-80 μM, HBPS: 0-2000 μM, HBP: 0-2000 μM), the concentration of DszD was 4.7 μg/mL, and the assays were run for up to 5 minutes. For DszC dose-response assays, NADH concentration was 500 μM, FMN concentration was 10 μM, DBT concentration was 5 μM, DszD concentration was 0.47 μg/mL, DszC concentration was 0.3 mg/mL, the concentration of the pathway intermediates was varied ($DBTO_2$: 0-80 μM, HBPS: 0-1000 μM, HBP: 0-2000 μM), and the assays were run for 10 min. For DszA dose-response assays, the NADH concentration was 500 μM, FMN concentration was 10 μM, $DBTO_2$ concentration was 80 μM, DszD concentration was 1.4 μg/mL, DszA concentration was 67 μg/mL, the concentration of the pathway intermediates was varied (DBT: 0-5 μM, HBPS: 0-500 uM, HBP: 0-1000 μM), and the

281 run time was 3 min. For DszB dose-response assays, HBPS concentration was 200 μM, the DszB
282 concentration was 58.5 μg/mL, the concentration of the pathway intermediates was varied (DBT:
283 0-5 μM, $DBTO_2$: 0-80 μM, HBP: 0-1000 μM), and the assays were run for 5 min.
284
285 *Analytical methods.* For DszD assays, the absorbance at 340 nm was measured using a
286 spectrophotometer to calculate the NADH concentration and this was used to calculate the
287 activity. The concentrations of DBT, $DBTO_2$, HBPS and HBP were measured using reversed
288 phase HPLC with a Zorbax SB-C18 column at a flow rate of 1 mL/min. For DszC and DszB
289 assays, the mobile phase was 50% acetonitrile-50% water and the temperature of the column was
290 maintained at 65°C. For DszA assays, the mobile phase was 30% acetonitrile-70% 10 mM
291 tetrabutylammonium bisulfate, 15 mM acetic acid pH 5.0 mobile phase and the temperature of
292 the column was maintained at 45°C.
293
294 **Results**
295 *Screening HBP-selective adsorbent resins.* A variety of commercially available resins were
296 screened for their ability to uptake HBP and DBT from a 0.50 vol/vol hexadecane-water solution
297 with an initial concentration of 10000 μM DBT and 10000 μM HBP in hexadecane. The resins
298 screened in this study were chosen because they span a wide range of resin hydrophobicity and
299 ionic functionalities, and most have been previously investigated in our lab (15). We found that
300 poly(styrene-*co*-DVB) derived resins generally have the greatest affinity for HBP (Figure 2A, X_r
301 = 10 g-resin/L-total for each resin). For instance, Dowex® Optipore L-493 and SD-2 were able
302 to achieve specific loadings of HBP of 40 and 50 mg/g-resin, respectively. In addition to having
303 the highest affinity for HBP of all the resins tested, Dowex® Optipore L-493 and SD-2 also

possessed the highest selectivity for HBP relative to DBT with HBP loadings that were 2.1 and 2.5 times greater than their respective DBT loadings. These resins were also found to have the highest affinity for butanol, with specific loadings of butanol of 175 and 150 mg/g-resin, respectively (15). The high affinity of these resins for butanol has been attributed to strong hydrophobic interactions between the resin's π-π bonds of the aromatic side groups and the alkyl chain of butanol and to the resin's high specific surface area (15). The affinity of these resins for HBP is likely due to strong hydrophobic interactions between the resin's aromatic side groups and the biphenyl part of HBP, though the specific loadings are reduced relative to n-butanol.

Four-component BDS experiments. We previously reported that the DBT desulfurization activity of *R. erythropolis* IGTS8 was significantly reduced as HBP accumulated in the medium during the BDS process (A. Abin-Fuentes, J.C. Leung, M.E.S Mohamed, D.I.C Wang, K.L.J. Prather, submitted for publication). In particular, we found that the activity of a resting cell suspension of 15.5 g DCW/L was decreased by 90% when the HBP concentration in the aqueous medium reached 40 μM (A. Abin-Fuentes, J.C. Leung, M.E.S Mohamed, D.I.C Wang, K.L.J. Prather, submitted for publication). In previous work, the use of Dowex® Optipore SD-2 in butanol fermentations led to a decrease in aqueous phase concentration and increase in productivity (15). In the current work, this resin, which had the best affinity and selectivity for HBP of all resins studied, was used to try to mitigate the reduction in biocatalyst activity correlated with HBP accumulation during the BDS process, thereby increasing the conversion of DBT. *R. erythropolis* IGTS8 resting cell suspensions of 15.5 g DCW/L were mixed with hexadecane (0.50 vol/vol) containing 10000 μM DBT and Dowex® Optipore SD-2 was added at X_r of 0, 10 or 50 g/L. The four-component (oil, water, cells and resin) mixtures were incubated

327 at 30°C in a rotary shaker at 250 RPM for 26 hours. The concentration of DBT and HBP in each
328 component was measured at the end of the incubation period. The partition coefficient of HBP
329 between one component (component 1) and another component (component 2) in the four-
330 component BDS experiments is expressed as:

331 $$P_{comp1/comp2} = \frac{C_{\mathrm{HBP,comp1}}}{C_{\mathrm{HBP,comp2}}}, \quad (5)$$

332 where $C_{HBP,comp1}$ is the measured HBP concentration in component 1 and $C_{HBP,comp2}$ is the
333 measured HBP concentration in component 2. For example, $P_{R/C}$ is the partition coefficient of
334 HBP between the resin and the biocatalyst (cells). Similarly, $P_{O/W}$ is the partition coefficient of
335 HBP between hexadecane (oil) and water. The partition coefficients calculated at the different
336 resin concentrations are shown in Table I. The resin Dowex Optipore® SD-2 had the highest
337 affinity for HBP relative to the other components of the system. This resin had log $P_{R/C}$ and log
338 $P_{R/O}$ values around 2, which means that the resin's affinity for HBP was around 100 times greater
339 than the affinity of either the hexadecane oil phase or the biocatalyst. Furthermore, this resin had
340 a log $P_{R/W}$ around 4, which means that its affinity for HBP was around 10,000 times greater than
341 that of the aqueous buffer. The partition coefficients of HBP between oil and the aqueous buffer
342 ($P_{O/W}$) and between the biocatalyst and the aqueous buffer ($P_{C/W}$) were very similar (Table I).
343 The log $P_{O/W}$ and log $P_{C/W}$ in the absence of resin were 1.7 and 1.8, respectively. Also, the
344 partition coefficient of HBP between the biocatalyst and oil ($P_{C/O}$) was calculated to be 1 in the
345 absence of resin. The finding that $P_{O/W} \approx P_{C/W}$ and $P_{C/O} \approx 1$ indicates that the oil and biocatalyst
346 components have very similar affinity for HBP. Both the oil and the biocatalyst have an affinity
347 for HBP that is 50-60 times greater than that of the aqueous buffer in the absence of resin (Table
348 I).

349 The partition coefficient $P_{C/W}$ is defined as:

$$P_{C/W} = \frac{C_{\text{HBP, intracellular}}}{C_{\text{HBP, water}}}, \quad (6)$$

where $C_{HBP,water}$ is the HBP concentration in the water phase and $C_{HBP,intracellular}$ is the HBP concentration within the biocatalyst. The cell can be viewed as being composed of two components: the inner cytoplasmic space and the outer envelope/shell that encompasses the cytoplasm, which is the cell wall. The partition coefficient of HBP between the cytoplasm and water ($P_{cytoplasm/W}$) was estimated from solving for its value in the expression:

$$P_{C/W} = P_{\text{cell wall/W}} f_{\text{cell wall}} + P_{\text{cytoplasm/W}} f_{\text{cytoplasm}} \quad (7)$$

where $P_{cell\ wall/W}$ is the partition coefficient of HBP between the cell wall and the water. The value of $P_{cell\ wall/W}$ was estimated to be 550 (see Supplemental Material). $f_{cell\ wall}$ and $f_{cytoplasm}$ are the fractions of the total volume of a single cell that are occupied by the cell wall and cytoplasm, respectively. The values of $f_{cytoplasm}$ and $f_{cell\ wall}$ were calculated from the expressions:

$$f_{cytoplasm} = \frac{\left(R_{cell} - W\right)^3}{\left(R_{cell}\right)^3} \quad (8)$$

$$f_{\text{cell wall}} = 1 - \frac{\left(R_{cell} - W\right)^3}{\left(R_{cell}\right)^3}, \quad (9)$$

where W is the thickness of the cell wall, which has been estimated to be approximately 10 nm for *Rhodococcous* species (16). R_{cell} is the radius of the cell, which was estimated to be 0.5 μm (17). The cytoplasmic HBP concentration ($C_{HBP,cytoplasm}$) was calculated from the following expression:

$$C_{\text{HBP, cytoplasm}} = P_{\text{cytoplasm/W}}\, C_{\text{HBP,water}} \quad (10)$$

372 The value of $C_{HBP,cytoplasm}$ was calculated to be 1100, 330 and 260 μM at resin concentrations (X_r)
373 of 0, 10 and 50 g/L, respectively (Figure 2B). The corresponding HBP loadings on the
374 biocatalyst (L_c) were calculated to be 1.6, 0.5 and 0.2 mg HBP/g DCW using equation 3 (Figure
375 2B). These values show that the resin was effective in reducing HBP retention within the
376 cytoplasm of the biocatalyst, which is where the desulfurization enzymes are present (4).
377 Despite the significant decrease in HBP retained within the cytoplasm, the total amount of HBP
378 produced in the system did not increase with increasing resin concentration (Figure 2B).
379 Therefore, it was postulated that the biocatalyst, and in particular the desulfurization enzymes,
380 might be susceptible to cytoplasmic HBP concentrations smaller than 260 μM.
381
382 *Enzyme kinetics.* To study the kinetics of each enzyme, recombinant protein was expressed in
383 and purified from *E. coli* (See Supplemental Material). For DszA, DszB and DszD, the kinetic
384 data obtained was appropriately modeled by the Michaelis-Menten model (Figure 3A, 3B, 3D).
385 The equation for this model is:

386 $$\nu = \frac{k_{cat}[E_0][S]}{K_m + [S]} = \frac{V_{\max}[S]}{K_m + [S]}, \quad (11)$$

387 where ν is the enzyme activity, k_{cat} is the turnover number, $[E_0]$ is the enzyme concentration in
388 each assay, [S] is the substrate concentration and K_m is the Michaelis constant. The kinetics of
389 DszC could not be modeled accurately with a simple Michaelis-Menten model because it was
390 found that DszC was inhibited by its substrate DBT (Figure 3C). As a result, a substrate
391 inhibition model was used to fit the data obtained with DszC (18):

392 $$\nu = \frac{V_{\max}[S]}{K_m + [S] + \frac{[S]^2}{K_{SI}}}, \quad (12)$$

where K_{SI} is the substrate (DBT) inhibition constant.

The fitting of the models to the data was done using the *enzkin* package in MATLAB®. The kinetic data obtained for all four desulfurization enzymes is shown in Figure 3. The kinetic parameters of each enzyme are summarized in Table II and compared to parameters from other studies, where available. To our knowledge, the only prior detailed characterization of a desulfurization enzyme from *R. erythropolis* IGTS8 found k_{cat} = 1.3 ± 0.07 min^{-1} and K_m = 0.90 ± 0.15 μM for DszB (6). In the current work, kinetic characterization of DszB yielded k_{cat} = 1.7 ± 0.2 min^{-1} and K_m = 1.3 ± 0.3 μM, which are in good agreement with values from the previous study. Rough preliminary characterization of DszA and DszD from *R. erythropolis* IGTS8 yielded k_{cat} values of "about 60 min^{-1}" and approximately 300 min^{-1}, respectively (4). The corresponding values of k_{cat} for DszA and DszD measured in this work were 11 ± 2 min^{-1} and 760 ± 10 min^{-1}, which are of the same order of magnitude as those rough estimates from preliminary characterization studies. DszC was inhibited by its substrate DBT and the kinetic parameters obtained were k_{cat} = 1.6 ± 0.3 min^{-1}, K_m = 1.4 ± 0.3 μM and K_{SI} = 1.8 ± 0.2 μM. The activity of DszC from *R. erythropolis* D-1 was reported as 30.3 nmole $DBTO_2$/mg DszC/min (19), which is in close agreement with the maximum activity measured in this work of 31.3 nmole $DBTO_2$/mg DszC/min (Figure 3C).

The catalytic efficiency of an enzyme is best defined by the ratio of the kinetic constants, k_{cat}/K_m (20). The catalytic efficiency of each desulfurization enzyme was calculated (Table II). The catalytic efficiencies of DszA, DszB, DszC were calculated to be 3.1, 1.3, 1.1 $\mu M^{-1}min^{-1}$, respectively. The catalytic efficiency of DszD on NADH and FMN was calculated to be 6.7 and 100 $\mu M^{-1}min^{-1}$, respectively. Therefore, the enzymes can be listed in order of decreasing efficiency as: DszD > DszA > DszB ≈ DszC.

416

417 *Identification of four major inhibitory interactions in the 4S pathway*. All of the possible
418 interactions among the 4 different desulfurization enzymes and the four compounds in the
419 pathway (DBT, $DBTO_2$, HBPS and HBP) were studied to determine the major inhibitory
420 interactions. DBTO was not included because it is not typically observed during the BDS
421 process because its rate of consumption is much faster than its rate of generation (4). The
422 strength of inhibition was studied by means of a dose-response plot. The dose-response equation
423 describing the effect of inhibitor concentration on enzyme activity is expressed as (20):

424 $$\frac{v_i}{v_0} = \frac{1}{1 + \frac{[I]}{IC_{50}}}, \qquad (13)$$

425 where v_i is the enzyme's activity at an inhibitor concentration of [I], v_0 is the enzyme's activity in
426 the absence of inhibitor, and IC_{50} is the concentration of inhibitor required to reduce the
427 enzyme's activity by 50%. The IC_{50} parameter is phenomenological and has no mechanistic
428 implications. The value of IC_{50} was obtained by fitting the data of v_i / v_0 versus [I] using the non-
429 linear fitting package *nlinfit* in MATLAB® to the dose-response equation. The four major
430 inhibitory interactions identified were (in order of decreasing strength): DszC inhibition by
431 HBPS (IC_{50} = 15 ± 2 μM), DszC inhibition by HBP (IC_{50} = 50 ± 5 μM), DszA inhibition by HBP
432 (IC_{50} = 60 ± 5 μM) and DszB inhibition by HBP (IC_{50} = 110 ± 10 μM) (Figure 4 and Table III).
433 Note that the IC_{50} values of all four inhibitory interactions are significantly smaller than the
434 estimated cytoplasmic HBP concentration. Even in the best-case scenario, when 50 g/L of a
435 highly HBP-selective resin was added to the BDS mixture, the estimated cytoplasmic HBP
436 concentration was still 260 μM. This finding suggests that these four inhibitory interactions are

likely responsible for the reduction in biocatalyst activity that is observed during a typical BDS process when HBP is generated endogenously from DBT within the biocatalyst.

The only prior preliminary characterization of inhibition within the 4S pathway showed that DszB from *R. erythropolis* KA2-5-1 had an IC_{50} of around 2000 μM with respect to HBP (12). We report here three new inhibitory interactions in the pathway that are stronger than any previous preliminary findings. Note that the strongest inhibitory interactions are on the first enzyme in the pathway, DszC, and the strength of inhibition decreases farther down the pathway, with the last enzyme in the pathway, DszB, having the weakest HBP inhibition at IC_{50} = 110 μM (Figure 4B). Note also that the major inhibitory compounds in the pathway are the last two intermediates, HBPS and HBP. This pattern of inhibition is typical of feedback inhibition of linear pathways; for example, in the tricarboxylic acid (TCA) cycle the first enzyme in the pathway is strongly inhibited by the end product ATP.

Mechanism of the major inhibitory interactions in the 4S pathway. The telltale sign of non-competitive inhibition is a reduced V_{max} without a change in K_m as the inhibitor concentration is increased (20). This phenomenon was observed in the inhibition of DszC by both HBPS and HBP (Figure 5A and Figure 5B). The model for non-competitive inhibition of an enzyme that obeys Michaelis-Menten kinetics is given by (20):

$$v = \frac{V_{\max}[S]}{K_m\left(1+\frac{[I]}{K_I}\right)+[S]\left(1+\frac{[I]}{\alpha K_I}\right)}, \qquad (14)$$

where [I] is the inhbitior concentration, K_i is the inhibition constant, and α is a parameter that reflects the effect of inhibitor on the affinity of the enzyme for its substrate, and likewise the

457 effect of the substrate on the affinity of the enzyme for the inhibitor. Non-competitive inhibition
458 refers to the case in which an inhibitor displays binding affinity for both the free enzyme and the
459 enzyme-substrate binary complex (see Supplemental Material). This form of inhibition is the
460 most general case; in fact, competitive and uncompetitive inhibition can be viewed as special,
461 restricted cases of non-competitive inhibition in which the value of α is infinity or zero,
462 respectively (20). Since the kinetics of DszC showed substrate inhibition, a modification to the
463 non-competitive model was derived (see Supplemental Material). The non-competitive
464 inhibition of DszC by HBPS and HBP can be expressed as:

465 $$v = \frac{V_{\max}[S]}{K_m\left(1+\frac{[I]}{K_I}\right)+[S]\left(1+\frac{[I]}{\alpha K_I}\right)+\frac{[S]^2}{K_{SI}}} \qquad (15)$$

466 The solid lines in Figures 5A and 5B represent the fits for the non-competitive inhibition model
467 (equation 15), where the values of K_i and α were 13.5 μM and 0.13 for HBPS inhibition and 40
468 μM and 0.4 for HBP. Fitting of the model to the data was attempted using *nlinfit* from
469 MATLAB®, but was unsuccessful due to convergence issues. Instead the parameters were
470 determined by a graphical method outlined in section 8.3 of (20). The first step in this method
471 was the construction of the double-reciprocal Lineweaver-Burk plot. To obain the values of K_i
472 and αK_i two secondary plots were constructed. The first of these was a Dixon plot of $1/V_{max}$ as a
473 function of [I], from which the value of $-\alpha K_i$ can be determined as the x-intercept. In the second
474 plot, the slopes of the double-reciprocal lines (from the Lineweaver-Burk plot) are plotted as a
475 function of [I]. For this plot, the x-intercept will be equal to $-K_i$. Combining the information
476 from these two secondary plots allows determination of both inhibition parameters. The

477 mechanism of DszB inhibition by HBP and DszA inhibition by HBPS could not be determined
478 due to limited resolution of the HPLC detector.
479
480 *Enzyme inhibition model predicts reduction in biocatalyst activity.* A model that
481 incorporated enzyme inhibition was developed to predict the volumetric desulfurization rate in
482 biphasic (oil-water) BDS experiments (See Supplemental Material for model equations). The
483 model accounted for DBT and HBP in three components: oil, water and cytoplasm. The two
484 pathway intermediates, $DBTO_2$ and HBPS, were assumed to only be present in the cytoplasm.
485 The three major inhibitory interactions by HBP on DszA, DszB and DszC were taken into
486 account. The fourth major inhibitory interaction, the inhibition of DszC by HBPS, was ignored
487 for simplicity. DszD activity was assumed to not be limiting and was therefore excluded from
488 the model. Loss of biocatalyst activity unrelated to HBP accumulation was also taken into
489 account in the model through an exponential decay constant, k_d (See Supplemental Material).
490 Concentrations of DszA, DszB and DszC were assumed to be all the same and equal to E_0. E_0
491 was the only floating parameter in the model. The value of E_0 was obtained by allowing its value
492 to vary until the initial desulfurization rate predicted by the model matched the measured
493 desulfurization rate. The value of E_0 obtained was 15 mg/mL, so that the total concentration of
494 desulfurization enzymes in the cytoplasm was 45 mg/mL. This value is of the same order as the
495 total cytoplasmic concentration of protein, which has been reported to be approximately 200
496 mg/mL (22).
497 The first step in the biphasic BDS experiments was growth of biocatalyst in a 4L
498 bioreactor to a cell density of 29-35 g DCW/L. Next, 10 % vol/vol hexadecane containing
499 100,000 μM DBT was added to the bioreactor. The desulfurization rate of DBT in the bioreactor

500 was monitored thereafter from the measured concentrations of DBT and HBP in the hexadecane
501 and aqueous phases. For the first two hours after hexadecane addition, the mixing speed was
502 maintained at 200 RPM. The mixing speed was increased to 500 RPM thereafter to minimize
503 mass transport limitations in the system. The enzyme inhibition model was used to predict the
504 desulfurization rate only after the shift in mixing speed to 500 RPM. The model predicts the
505 concentration of HBP in the oil and water phase and the volumetric desulfurization rate
506 accurately (Figures 6A, 6B and 6C). The coefficient of determination (R^2) between the model
507 and the data was calculated to be 0.96 using the MATLAB® function *corr(X,Y)*.

508

509 **Discussion**

510 Dose-response experiments were performed to investigate the potential inhibitory effect of the
511 various intermediates in the 4S pathway on the desulfurization enzymes. Four major inhibitory
512 interactions were identified, all of which had IC_{50} values under 110 μM. Three of the four major
513 inhibitory interactions were carried out by HBP. HBP was found to inhibit DszA, DszB and
514 DszC with IC_{50} values of 60, 110 and 50 uM, respectively. The fourth major inhibitory
515 interaction identified is the inhibition of DszC monooxygenase by HBPS. This interaction is the
516 strongest of the four since it has the lowest IC_{50} value of 15 μM. HBPS concentration during the
517 four-component BDS experiments was not measured in this work. The IC_{50} values of HBP on
518 the desulfurization enzymes are all significantly lower than the minimum cytoplasmic HBP
519 concentration estimated during the four-component BDS experiments, which was 260 μM. This
520 suggests that enzyme inhibition by HBP was responsible for the reduction in biocatalyst activity
521 during the four-component BDS experiments, even in the presence of 50 g/L of HBP-selective
522 resin (Dowex ® Optipore SD-2). In the n-butanol fermentation by *Clostridium acetobutylicum*

ATCC 824, n-butanol productivity was increased two-fold upon addition of Dowex® Optipore SD-2 to the medium (15). However, the n-butanol toxicity threshold of *Clostridium* is generally considered to be about 1.3% (wt./vol.), which is approximately 180 mM (15). The fact that the inhibitory levels of HBP on the *R. erythropolis* IGTS8 desulfurization enzymes are at least 3 orders of magnitude smaller than the toxicity levels of n-butanol on *Clostridium* might explain why n-butanol productivity by *Clostridium* was enhanced upon addition of Dowex ® Optipore SD-2 while HBP productivity by *R.erythropolis* IGTS8 was not enhanced.

In another study, *R. erythropolis* IGTS8 lysates were supplied with 200 μM DBT initially and the concentrations of DBT, $DBTO_2$, HBPS and HBP were monitored over time (4). After 10 minutes, all DBT was depleted, the HBPS concentration was approximately 130 μM and the HBP concentration was approximately 50 μM (4). From 10 to 60 minutes, the HBPS concentration decreased steadily from 130 to 0 μM and the HBP concentration increased from 50 to 200 μM. No $DBTO_2$ was detected at any time (4). All of these results agree with the kinetic data obtained in this work. First of all, since the k_{cat} of DszA is approximately 7 times that of DszC (Table II), $DBTO_2$ consumption rate is expected to be significantly greater than its generation rate, which agrees with the fact that no $DBTO_2$ was detected. Second, the buildup of HBPS within the first 10 min is consistent with the fact that its consumption rate (DszB k_{cat} = 1.7 min^{-1}) is significantly slower than its generation rate (DszA k_{cat} = 11.2 min^{-1}) (Table II). The fact that the HBP concentration accumulates to over 130 μM within the first few minutes indicates that DszC would have been severely inhibited by HBPS at that point in time. As HBPS is consumed, DszC inhibition by HBPS is relieved but then HBP inhibition of DszC (and DszA and DszB) become more significant. Therefore, we expect that during a BDS experiment all four major inhibitory interactions reported here would be important. HBPS inhibition of DszC is

546 responsible for maintaining the BDS rate low at the beginning of the BDS process when HBP
547 levels are still low. Once HBP levels rise, HBP inhibition of DszA, DszB and DszC will be
548 mostly responsible for inhibition of the BDS rate.

549 Due to the biocatalyst's high affinity for HBP relative to the aqueous buffer ($P_{C/W}$ = 60 at
550 X_r = 0 g/L), the intracellular HBP concentration ($C_{HBP,intracellular}$) is much higher than the HBP
551 concentration in the aqueous buffer ($C_{HBP,water}$). In previous studies, HBP inhibition in biphasic
552 (oil-water) BDS experiments has been downplayed due to the partition coefficient of HBP
553 between oil and water ($P_{O/W}$) being high (around 40-50) (23). It has been generally assumed that
554 since the biocatalyst resides in the aqueous phase, the intracellular concentration of HBP is
555 similar to the aqueous phase concentration. This assumption is in part because the biocatalyst's
556 affinity for HBP has not been quantified in previous studies. We have shown that this affinity
557 for HBP is in par with that of the oil phase. As a result, HBP retention within the biocatalyst and
558 HBP inhibition of the desulfurization enzymes is an obstacle even in biphasic BDS experiments.

559 The affinity of the biocatalyst for HBP is an intrinsic property of the biocatalyst and will
560 likely vary depending on the biocatalyst employed. Interactions between cyclic hydrocarbons
561 and biological membranes have been previously investigated (24). The partition coefficients of a
562 range of cyclic hydrocarbons (including aromatics) between liposomes prepared from *E. coli*
563 phospholipids and an aqueous phosphate buffer were measured. From these measured partition
564 coefficients, a correlation for predicting the partition coefficient of any cyclic hydrocarbon
565 between the liposome (membrane) and the aqueous buffer ($P_{M/B}$) based on the octanol-water
566 partition coefficient ($P_{O/W}$) of that cyclic hydrocarbon was developed. The liposome-buffer
567 partition coefficient of HBP is predicted to be $\log(P_{M/B}) = 2.2$ given the known value of the
568 octanol-water partition coefficient $\log(P_{O/W}) = 3.09$ (25). This is in good agreement with the

569 value of the partition coefficient of HBP between the biocatalyst and the buffer measured in this
570 work of log($P_{C/W}$) = 1.8-2.2 (Table I). The liposomes prepared by Sikkema et al (1994) are
571 representative of the cytoplasmic membrane of a gram-negative bacterium. *R. erythropolis*,
572 being a gram-positive bacteria, has a thin cytoplasmic membrane surrounded by a thick cell wall
573 made mostly of peptidoglycan sturcutre and mycolic acids (10). The fact that the value of
574 log($P_{C/W}$) measured in this study agrees well with the predicted value of log($P_{M/B}$) suggests that
575 HBP retained by *R. erythropolis* IGTS8 might reside mostly within the cytoplasmic membrane as
576 opposed to the cell wall, which is structurally very different. This idea agrees with the
577 mechanism of DBT to HBP conversion during the BDS process. When DBT is added
578 exogenously, it is transported into the cell (likely by passive diffusion). Inside the cytoplasm, the
579 DBT is transformed to HBP via the 4S pathway and then the HBP will interact first with the
580 cytoplasmic membrane as it attempts to exit the cell.
581
582 **Conclusions**
583 In this work, the mechanism of biocatalyst inhibition in the BDS of DBT was investigated.
584 Retention of the final product HBP during the BDS process to concentrations in the hundreds of
585 μM range or higher leads to inhibition of the three enzymes in the linear part of the 4S pathway.
586 These three enzymes DszA, DszB and DszC have IC_{50} values with respect to HBP of 60, 110
587 and 50 μM, respectively. Host engineering to reduce retention of HBP might mitigate inhibition
588 of the 4S pathway by HBP. This poses a formidable challenge as it has been suggested that the
589 cytoplasmic membrane, which is ubiquitous in nature, may be responsible for HBP retention
590 within the biocatalyst. Protein engineering might also be explored as a means to overcome
591 inhibition of the pathway enzymes.

Acknowledgements

AAF was supported by the Biotechnology Training Program from the National Institute of Health (NIH). Research support from Saudi Aramco is also gratefully acknowledged. Dr. Christine Nguyen is gratefully acknowledged for synthesizing HBPS.

Nomenclature

C_{HBP} – concentration of HBP (μM)

$[E_0]$ – total enzyme concentration

$f_{cytoplasm}$ – volume fraction of a single cell occupied by cytoplasm

$f_{cell\ wall}$ – volume fraction of a single cell occupied by cell wall

[I] – Inhibitor concentration (μM)

IC_{50} – inhibitor concentration that reduces enzyme's activity by 50%

k_{cat} – enzyme turnover number (min^{-1})

K_m – Michaelis constant (μM)

K_{SI} – substrate inhibition constant (μM)

K_i – enzyme inhibition constant

L_c – loading of HBP on the cells (mg HBP/g DCW)

L_r – loading of HBP on resin (mg HBP/g resin)

m_c – mass of cells (g DCW)

m_r – mass of resin (g)

$P_{O/W}$ – HBP partition coefficient between hexadecane and aqueous buffer

$P_{C/W}$ – HBP partition coefficient between biocatalyst and aqueous buffer

$P_{R/W}$ – HBP partition coefficient between resin and aqueous buffer

$P_{C/O}$ – HBP partition coefficient between biocatalyst and hexadecane

$P_{R/C}$ – HBP partition coefficient between resin and biocatalyst

$P_{R/O}$ – HBP partition coefficient between resin and hexadecane

$P_{cell\ wall/W}$ – HBP partition coefficient between the cell wall and aqueous buffer

$P_{cytoplasm/W}$ – HBP partition coefficient between cytoplasm and aqueous buffer

620 R_{cell} – radius of the cell (μm)

621 [S] – Substrate concentration (μM)

622 V_{total} – total volume of oil, water and resin in HBP adsorption by resin experiments (L)

623 V_{max} – maximum enzyme activity (nmole product/g enzyme/min)

624 W – thickness of the cell wall (nm)

625 X_r – resin concentration (g/L)

626 α – parameter that reflects effect of inhibitor on enzyme's affinity for its substrate

627 ν_0 – enzyme's activity in the absence of inhibitor (nmole product/g enzyme/min)

628

629

630 **References**

631 1. Soleimani M, Bassi A, Margaritis A. 2007. Biodesulfurization of refractory organic
632 sulfur compounds in fossil fuels. Biotech. Adv. 25: 570-596.
633 2. Kilbane JJ. 2006. Microbial biocatalyst developments to upgrade fossil fuels. Curr. Opin.
634 Biotechnol. 17:305–314
635 3. Gray KA, Mrachko GT, Squires CH. 2003. Biodesulfurization of fossil fuels. Curr. Opin.
636 Microbiol. 6:229–235
637 4. Gray KA, Pogrebinsky OS, Mrachko GT, Xi L, Monticello DJ, Squires CH. 1996.
638 Molecular mechanisms of biocatalytic desulfurization of fossil fuels. Nat. Biotech. 14:
639 1705-1709
640 5. Xi L, Squires CH, Monticello DJ, Childs JD. 1997. A flavin reductase stimulates DszA
641 and DszC proteins of *Rhodococcus erythropolis* IGTS8 in vitro. Biochem. Biophys. Res.
642 Commun. 230:73-75
643 6. Watkins LM, Rodriguez R, Schneider D, Broderick R, Cruz M, Chambers R, Ruckman
644 E, Cody M, Mrachko GT. 2003. Purification and characterization of the aromatic
645 desulfinase 2-(2'-hydroxyphenyl)benzenesulfinate desulfinase. Biochem. Biophys.
646 415:14-23
647 7. Schilling BM, Alvarez LM, Wang DIC, Cooney CL. Continuous desulfurization of
648 dibenzothiophene with *R. rhodochrous* IGTS8 (ATCC 53968). Biotechnol. Prog.
649 18:1207–1213.
650 8. Naito M, Kawamoto T, Fujino K, Kobayashi M, Maruhashi K, Tanaka A. 2001. Long-
651 term repeated desulfurization by immobilized *Rhodococcus erythropolis* KA2-5-1 cells.
652 Appl. Microbiol. Biotechnol. 55:374–378.

9. Jia X, Wen J, Sun Z, Caiyin Q, Xie S. 2006. Modeling of DBT biodegradation behaviors by resting cells of *Gordonia* sp.WQ-01 and its mutant in oil–water dispersions. Chem. Eng. Sci. 61: 1987 – 2000
10. Lichtinger T, Reiss G, Benz R. 2000. Biochemical identification and biophysical characterization of a channel-forming protein from *Rhodococcus erythropolis.* J. Bacteriol. 182(3): 764-770.
11. Honda H, Sugiyama H, Saito I, Kobayashi T. 1998. High cell density culture of Rhodococcus rhodochrous by pH-stat feeding and dibenzothiophene degradation. J. Ferment. Bioeng. 85: 334 –338.
12. Nakayama N, Matsubara T, Ohshiro T, Moroto Y, Kawata Y, Koizumi K, Hirakawa Y, Suzuki M, Maruhashi K, Izumi Y, Kurane R. 2002. A novel enzyme, 2′-hydroxybiphenyl-2-sulfinate desulfinase (DszB), from a dibenzothiophene-desulfurizing bacterium *Rhodococcus erythropolis* KA2-5-1: gene overexpression and enzyme characterization. Biochim. Biophys. Acta 1598:122–130.
13. Caro A, Boltes K, Leton P, Garcia-Calvo E. 2008. Description of by-product inhibition effects on biodesulfuriation of dibenzothiophene in biphasic media. Biodegradation 19: 599-611.
14. Chen H, Zhang WJ, Cai YB, Zhang Y, Li W. 2008. Elucidation of 2-hydroxybiphenyl effect on dibenzothiophene desulfurization by Microbacterium sp. strain ZD-M2. Biores. Tech. 99:6928-33.
15. Nielsen DR, Prather KJ. 2009. In situ product recovery of n-butanol using polymeric resins. Biotechnol. Bioeng. 102(3): 811-821
16. Sutcliffe IC, Brown AK, Dover LG. 2010. The rhodococcal cell envelope: composition,

organization and biosynthesis. Biology of Rhodococcus. Microbiology Monographs 16. Springer-Verlag Berlin Heidelberg.

17. Kilbane JJ. 1992. Mutant microorganisms useful for cleavage of organic C-S bonds. US patent 5,104,801.
18. Shuler ML, Kargi F . 2002. Bioprocess Engineering: Basic concepts. Second Edition. Prentice Hall, Inc.
19. Ohshiro T, Suzuki K, Izumi Y. 1997. Dibenzothiophene (DBT) degrading enzyme responsible for the first step of DBT desulfurization by *Rhodococcus erythropolis* D-1: Purification and characterization. J. Biosci. Bioeng. 83(3):233-237.
20. Copeland RA. 2000. Enzymes: a practical introduction to structure, mechanism, and data analysis. Second edition. Wiley-VCH p. 397
21. Matsubara T, Ohshiro T, Nishina Y, Izumi Y. 2001. Purification, characterization, and overexpression of flavin reductase involved in dibenzothiophene desulfurization by *Rhodococcus erythropolis* D-1. Appl. Environ. Microbio. 67(3):1179-1184
22. Ellis RJ. 2001. Macromolecular crowding: obvious but underappreciated. Trends Biochem. Sci. 26(10): 597-604
23. Caro A, Boltes K, Leton P, Garcia-Calvo E. 2007. Dibenzothiophene biodesulfurization in resting cell conditions by aerobic bacteria. J. Biochem. Eng. 35(2): 191-197
24. Sikkema J, de Bont JAM, Poolman B. 1994. Interactions of cyclic hydrocarbons with biological membranes. J. Bio. Chem. 269(11):8022-8028.
25. Hansch C, Leo A, Hoekman D. 1995. Exploring QSAR. Washington DC: American Chemical Society. P. 97

Tables

Table I. Comparison of partition coefficients between the four different components in the four component BDS experiments in the presence of the resin Dowex® Optipore SD-2.

Resin concentration (g/L)	$P_{C/O}$	$P_{C/W}$	$P_{O/W}$	$P_{R/C}$	$P_{R/O}$	$P_{R/W}$
0	1	60	52	-	-	-
10	1	47	42	88	99	4116
50	3	160	54	99	296	15906
Resin concentration (g/L)	log $P_{C/O}$	log $P_{C/W}$	log $P_{O/W}$	log $P_{R/C}$	log $P_{R/O}$	log $P_{R/W}$
0	0.1	1.8	1.7	-	-	-
10	0.0	1.7	1.6	1.9	2.0	3.6
50	0.5	2.2	1.7	2.0	2.5	4.2

C – cells
O – oil
W – water
R – resin

Table II. Summary of the main properties of the Dsz enzymes purified in this work including the molecular weight (MW), stock concentration and measured kinetic constants.

			This work			**Other authors**	
Enzyme	**M_w (kDa)**	**Stock Concentration (mg/mL)**	**k_{cat} (min^{-1})**	**K_m (µM)**	**k_{cat}/K_m (μM^{-1} min^{-1})**	**k_{cat} (min^{-1})**	**K_m (µM)**
DszA	49.6	1.3	11±2	3.6 ± 0.5	3.1	"about 60"[a]	"approx. 1"[a]
DszB	39.0	1.2	1.7±0.2	1.3 ± 0.3	1.3	1.3 ± 0.07 [b]	0.90 ± 0.15 [b]
DszC	45.0	6.1	1.6±0.3	1.4 ± 0.3, K_{SI} = 3 ± 0.2 µM	1.1	n/a	"less than 5"[a]
DszD	25.0	4.7	760±10	114 ± 5 (NADH), 7.3 ± 0.5 (FMN)	6.7 (NADH), 100 (FMN)	~300 [c]	208 (NADH), 10.8 (FMN) [d]

[a] Strain used was *R. erythropolis* IGTS8 (4)
[b] Strain used was *R. erythropolis* IGTS8 (6)
[c] Calculated estimate based on data in (4). Strain used was *R. erythropolis* IGTS8
[d] Strain used was *R. erythropolis* D-1 (21)

Table III. Summary of inhibition parameters for the four major inhibitory interactions including the mechanism of inhibition, the K_I, α and IC_{50} values.

Enzyme	**Inhibitor**	**Mechanism**	**K_I (µM)**	**α**	**IC_{50} (µM)**
DszA	HBP	Not determined	n/a	n/a	60 ± 5
DszB	HBP	Not determined	n/a	n/a	110 ± 10
DszC	HBPS	Non-competitive	13.5	0.13	15 ± 2
DszC	HBP	Non-competitive	40	0.4	50 ± 5

705 **Figure Captions**

706 **Figure 1.** The four-step biodesulfurization 4S pathway. The first two steps, catalyzed by both
707 DszC and DszD, are the conversion of DBT to DBT-sulfoxide (DBTO) and then to DBT-sulfone
708 ($DBTO_2$). The third step, catalyzed by both DszA and DszD, is the conversion of $DBTO_2$ to
709 HBPS. The final step is the conversion of HBPS to HBP by DszB.

710

711 **Figure 2**. (A) – Specific loading of HBP (white) and DBT (black) by the various resins tested at
712 a resin concentration of 10 g/L from a 0.50 vol./vol. hexadecane-water solution containing 10
713 mM DBT and 10 mM HBP initially. (B) – Total HBP produced (white) and cytoplasmic HBP
714 concentration (black) in four-component BDS experiment at 15.5 g DCW/L, oil fraction 0.50
715 vol/vol and 10 mM DBT. Specific HBP loadings are shown above black columns. Data shown
716 are the average and standard deviations of 3 replicates.

717

718 **Figure 3.** Enzyme kinetics for DszA (A), DszB (B), DszC (C), and DszD (D). Diamonds
719 represent data and solid lines represent Michaelis-Menten model fits for DszA, DszB and DszD
720 and substrate inhibition model for DszC. Data shown are the average and standard deviations of
721 3 replicates.

722

723 **Figure 4.** Normalized desulfurization enzyme activity at different inhibitor concentrations for
724 the four major inhibitory interactions identified in the 4S pathway. (A) – DszA inhibition by
725 HBP has an IC_{50} of 60 ± 5 μM; (B) – DszB inhibition by HBP has an IC_{50} of 110 ± 10 μM; (C) –
726 DszC inhibition by HBPS has an IC_{50} of 15 ± 2 μM; (D) – DszC inhibition by HBP has an IC_{50}
727 of 50 ± 5 μM. Data shown are the average and standard deviations of 3 replicates.

Figure 5. Non-competitive inhibition of DszC by HBPS and HBP. (A) – DszC activity at a range of DBT substrate concentrations from 0-5 μM and HBPS concentrations of 0 μM (closed diamonds), 5 μM (closed squares), 25 μM (closed triangles) and 50 μM (crosses). (B) – DszC activity at a range of DBT substrate concentrations from 0-5 μM and HBP concentrations of 0 μM (closed diamonds), 100 μM (closed squares), 500 μM (closed triangles). Solid lines are model fits from equation 15.

Figure 6. Enzyme inhibition model predictions for BDS bioreactor experiment. (A) – Volumetric desulfurization rate data (circles) and model prediction (line). (B) – Concentration of HBP in the oil phase data (circles) and model (line). (C) – Concentration of HBP in the water phase data (circles) and model (line). Data shown are the average and standard deviations of 3 replicates.

742 **Figures**

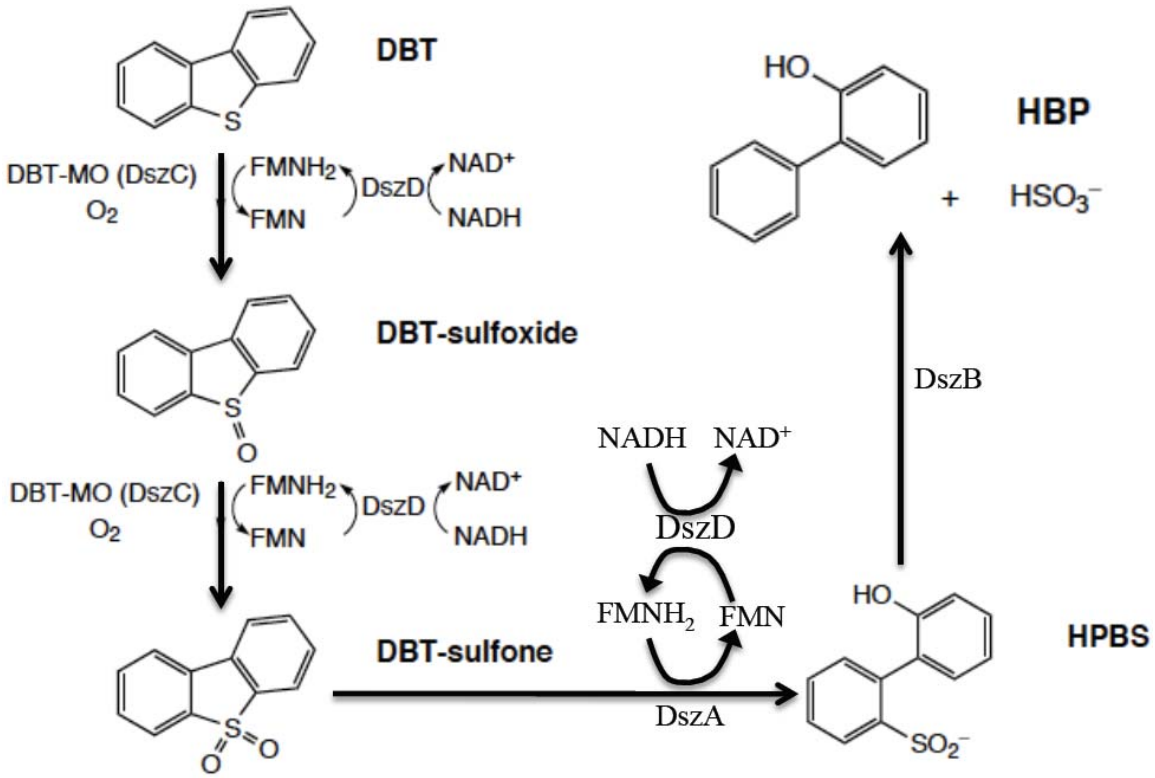

Figure 1. The four-step biodesulfurization 4S pathway. The first two steps, catalyzed by both DszC and DszD, are the conversion of DBT to DBT-sulfoxide (DBTO) and then to DBT-sulfone ($DBTO_2$). The third step, catalyzed by both DszA and DszD, is the conversion of $DBTO_2$ to HBPS. The final step is the conversion of HBPS to HBP by DszB.

743

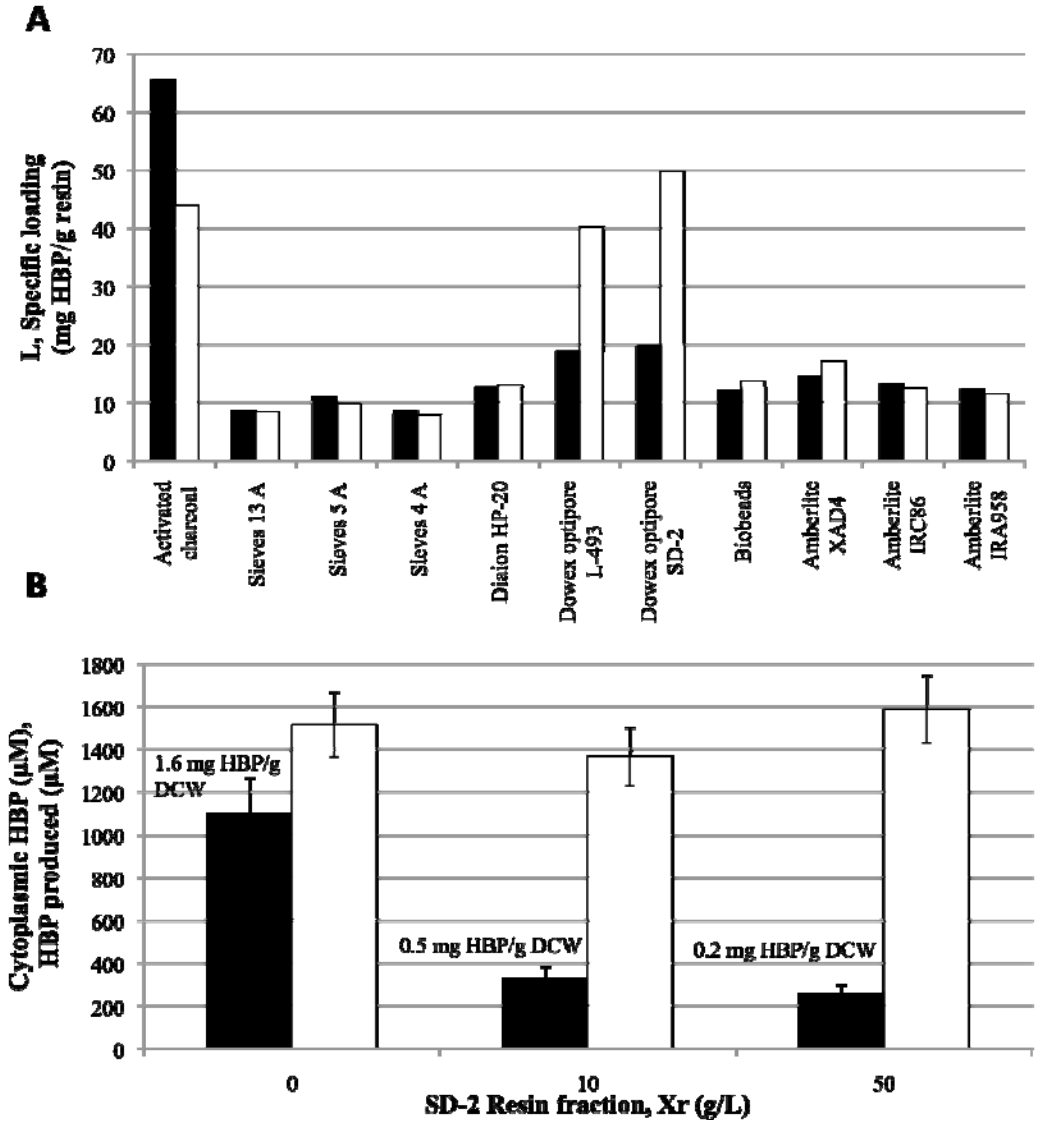

Figure 2. (A) – Specific loading of HBP (white) and DBT (black) by the various resins tested at a resin concentration of 10 g/L from a 0.50 vol./vol. hexadecane-water solution containing 10 mM DBT and 10 mM HBP initially. (B) – Total HBP produced (white) and cytoplasmic HBP concentration (black) in four-component BDS experiment at 15.5 g DCW/L, oil fraction 0.50 vol/vol and 10 mM DBT. Specific HBP loadings are shown above black columns. Data shown are the average and standard deviations of 3 replicates.

744

745

746

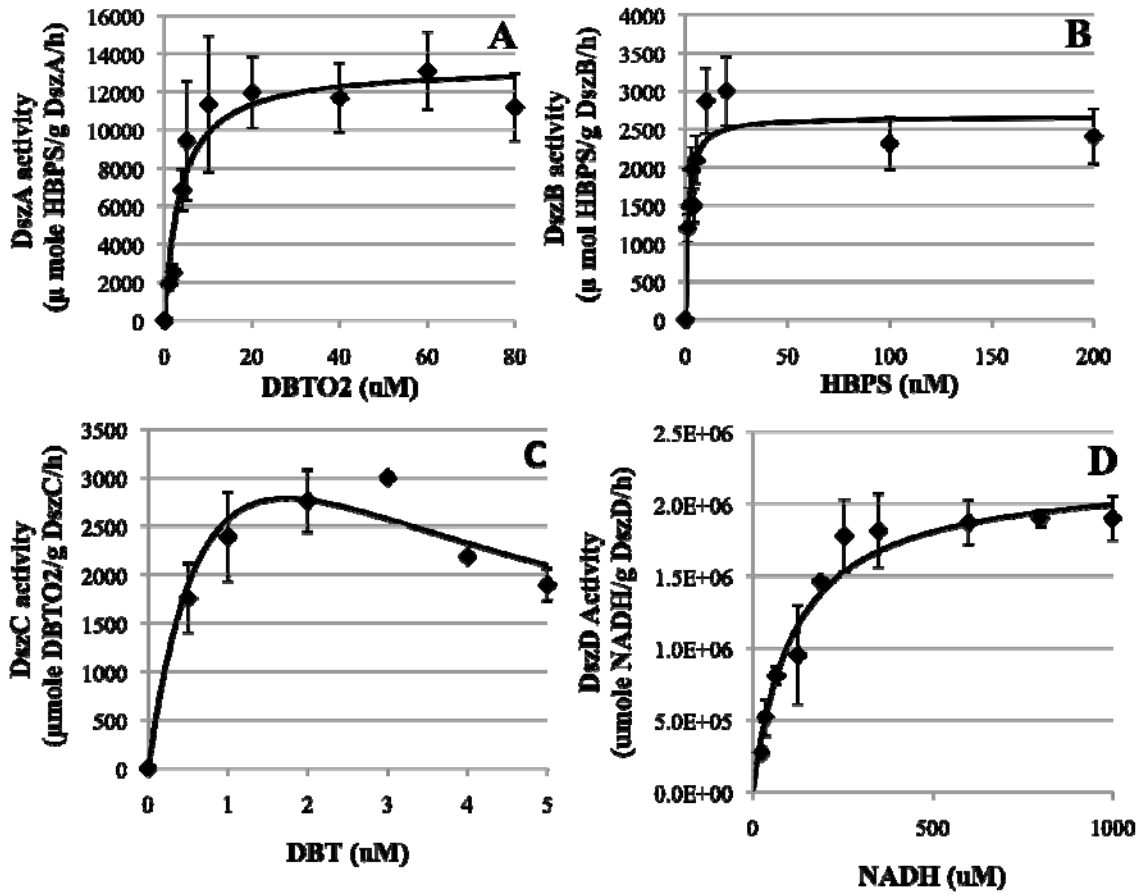

Figure 3. Enzyme kinetics for DszA (A), DszB (B), DszC (C), and DszD (D). Diamonds represent data and solid lines represent Michaelis-Menten model fits for DszA, DszB and DszD and substrate inhibition model for DszC. Data shown are the average and standard deviations of 3 replicates.

747

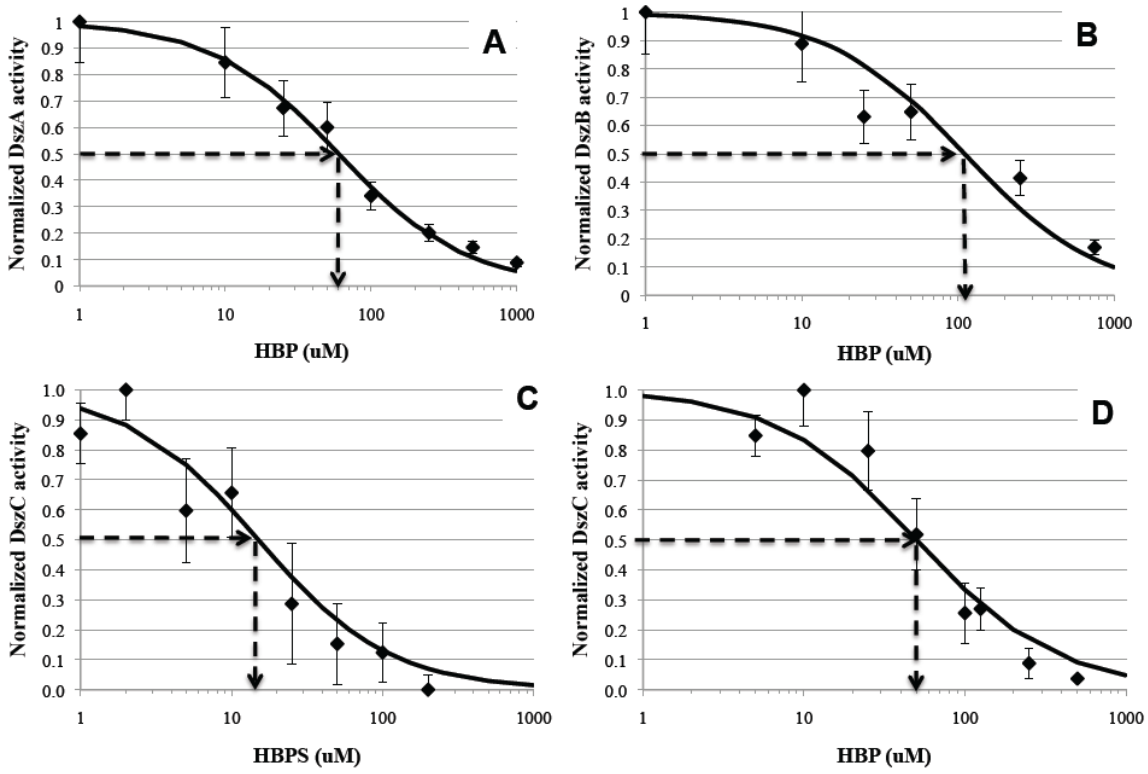

Figure 4. Normalized desulfurization enzyme activity at different inhibitor concentrations for the four major inhibitory interactions identified in the 4S pathway. (A) – DszA inhibition by HBP has an IC_{50} of 60 ± 5 μM; (B) – DszB inhibition by HBP has an IC_{50} of 110 ± 10 μM; (C) – DszC inhibition by HBPS has an IC_{50} of 15 ± 2 μM; (D) – DszC inhibition by HBP has an IC_{50} of 50 ± 5 μM. Data shown are the average and standard deviations of 3 replicates.

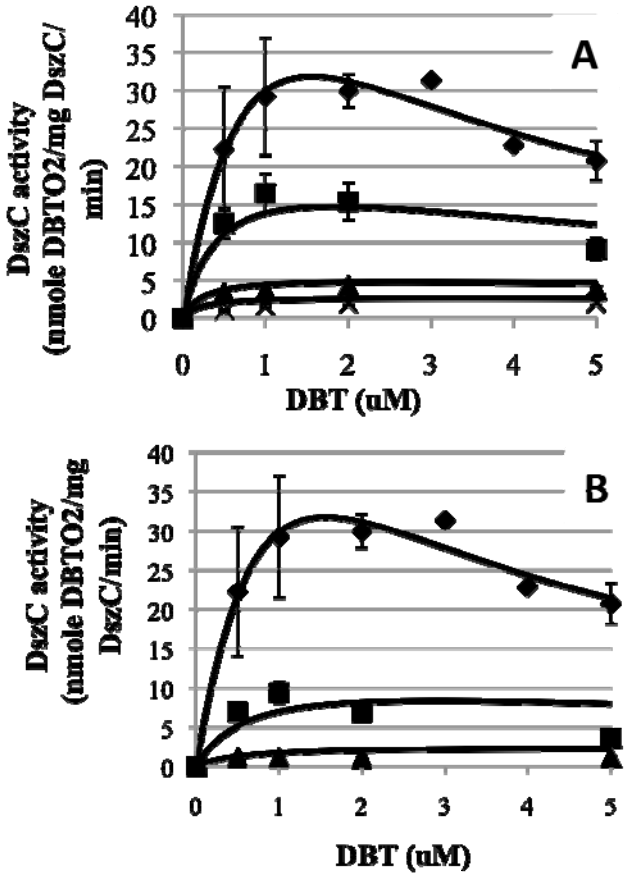

Figure 5. Non-competitive inhibition of DszC by HBPS and HBP. (A) – DszC activity at a range of DBT substrate concentrations from 0-5 μM and HBPS concentrations of 0 μM (closed diamonds), 5 μM (closed squares), 25 μM (closed triangles) and 50 μM (crosses). (B) – DszC activity at a range of DBT substrate concentrations from 0-5 μM and HBP concentrations of 0 μM (closed diamonds), 100 μM (closed squares), 500 μM (closed triangles). Solid lines are model fits from equation 15.

757

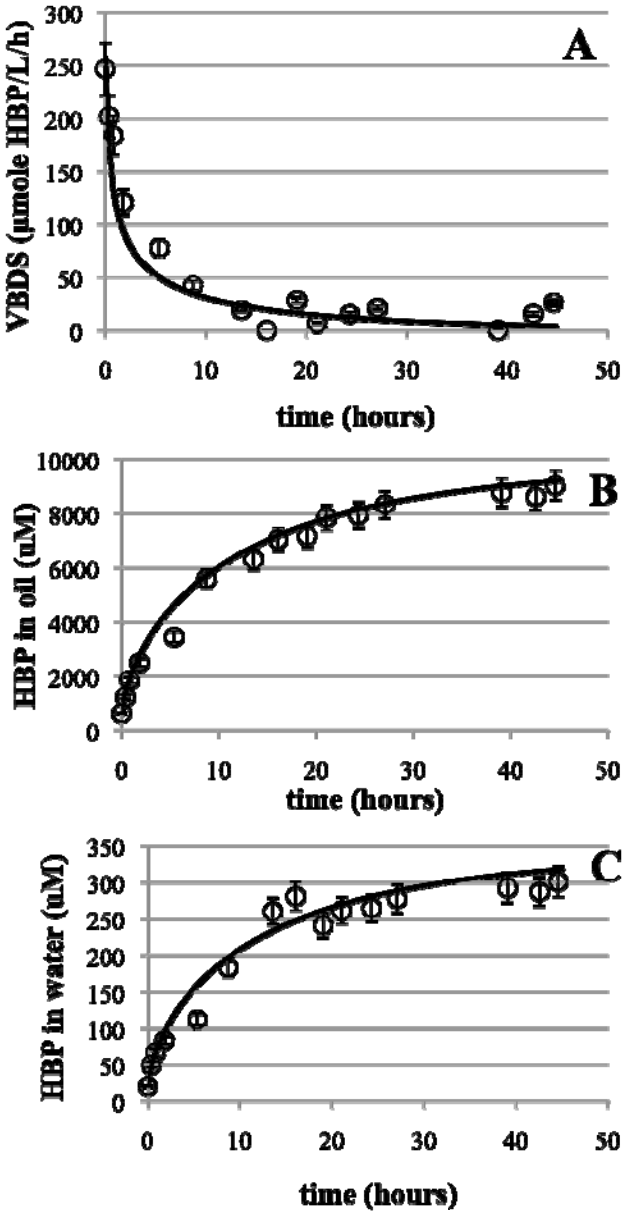

Figure 6. Enzyme inhibition model predictions for BDS bioreactor experiment. (A) – Volumetric desulfurization rate, V_{BDS}, data (circles) and model prediction (line). (B) – Concentration of HBP in the oil phase data (circles) and model (line). (C) – Concentration of HBP in the water phase data (circles) and model (line). Data shown are the average and standard deviations of 3 replicates.

758

759

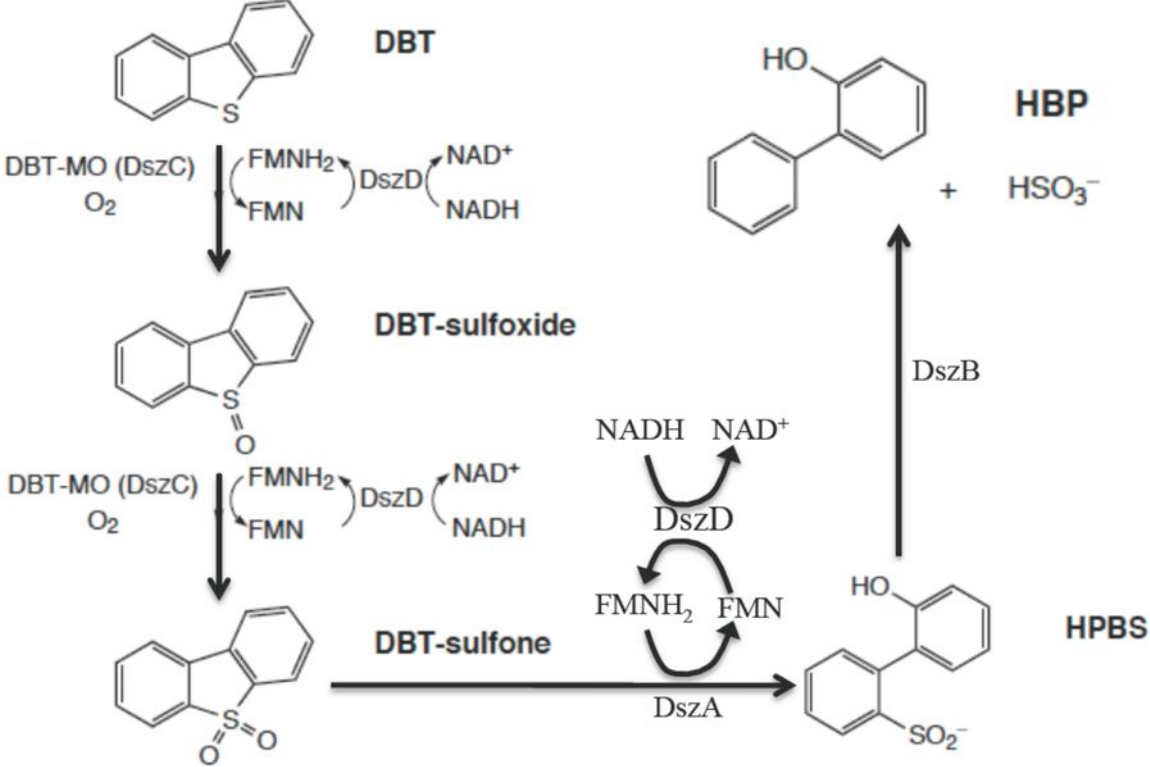
DBT
DBT-MO (DszC)
O2
FMNH2
FMN
DszD
NAD+
NADH
DBT-sulfoxide
DBT-MO (DszC)
O2
FMNH2
FMN
DszD
NAD+
NADH
DBT-sulfone
NADH
NAD+
DszD
FMNH2
FMN
DszA
HO
HPBS
SO2−
DszB
HO
HBP
+
HSO3−

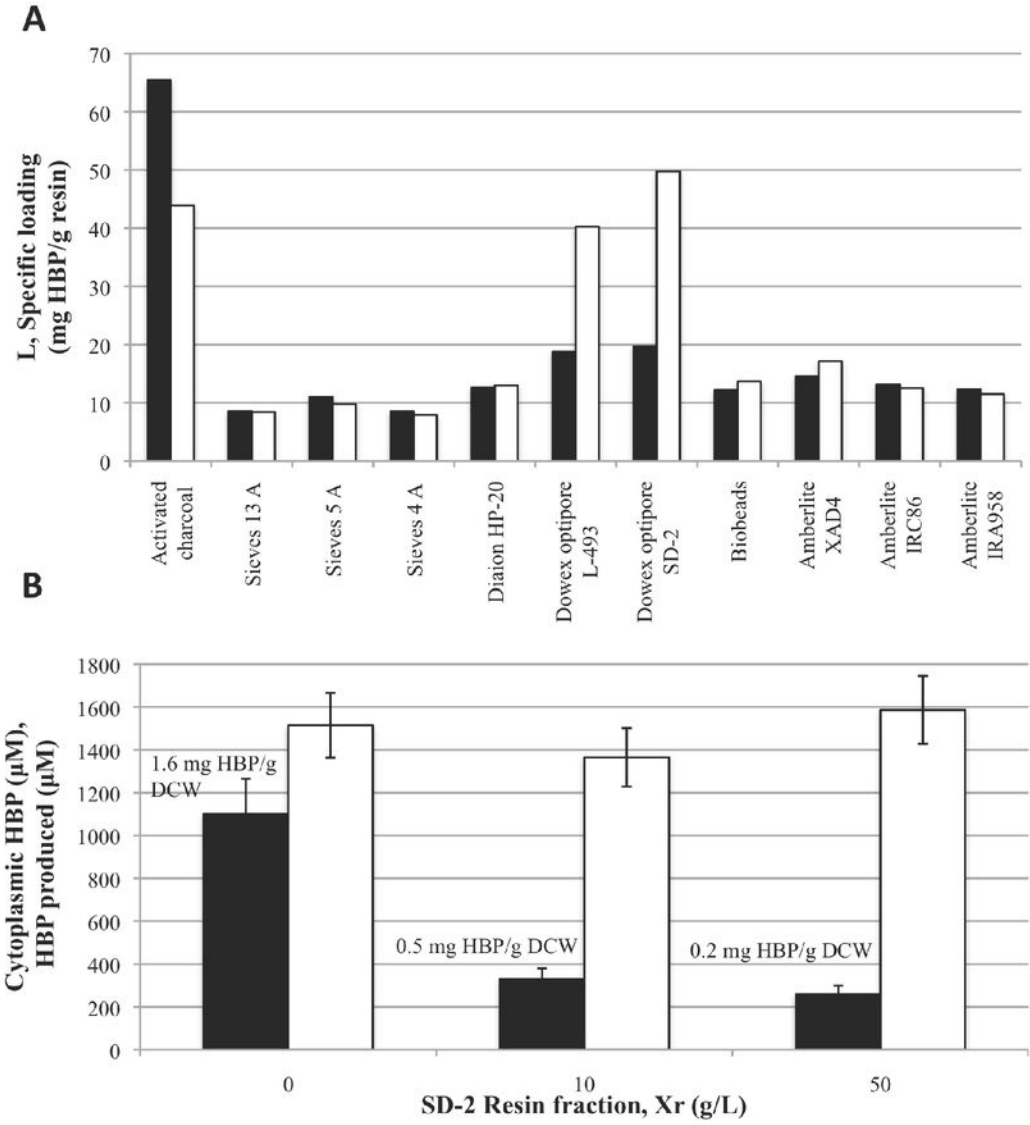
A
L, Specific loading (mg HBP/g resin)
70
60
50
40
30
20
10
0
Activated charcoal
Sieves 13 A
Sieves 5 A
Sieves 4 A
Diaion HP-20
Dowex optipore L-493
Dowex optipore SD-2
Biobeads
Amberlite XAD4
Amberlite IRC86
Amberlite IRA958
B
Cytoplasmic HBP (µM), HBP produced (µM)
1800
1600
1400
1200
1000
800
600
400
200
0
1.6 mg HBP/g DCW
0.5 mg HBP/g DCW
0.2 mg HBP/g DCW
0
10
50
SD-2 Resin fraction, Xr (g/L)

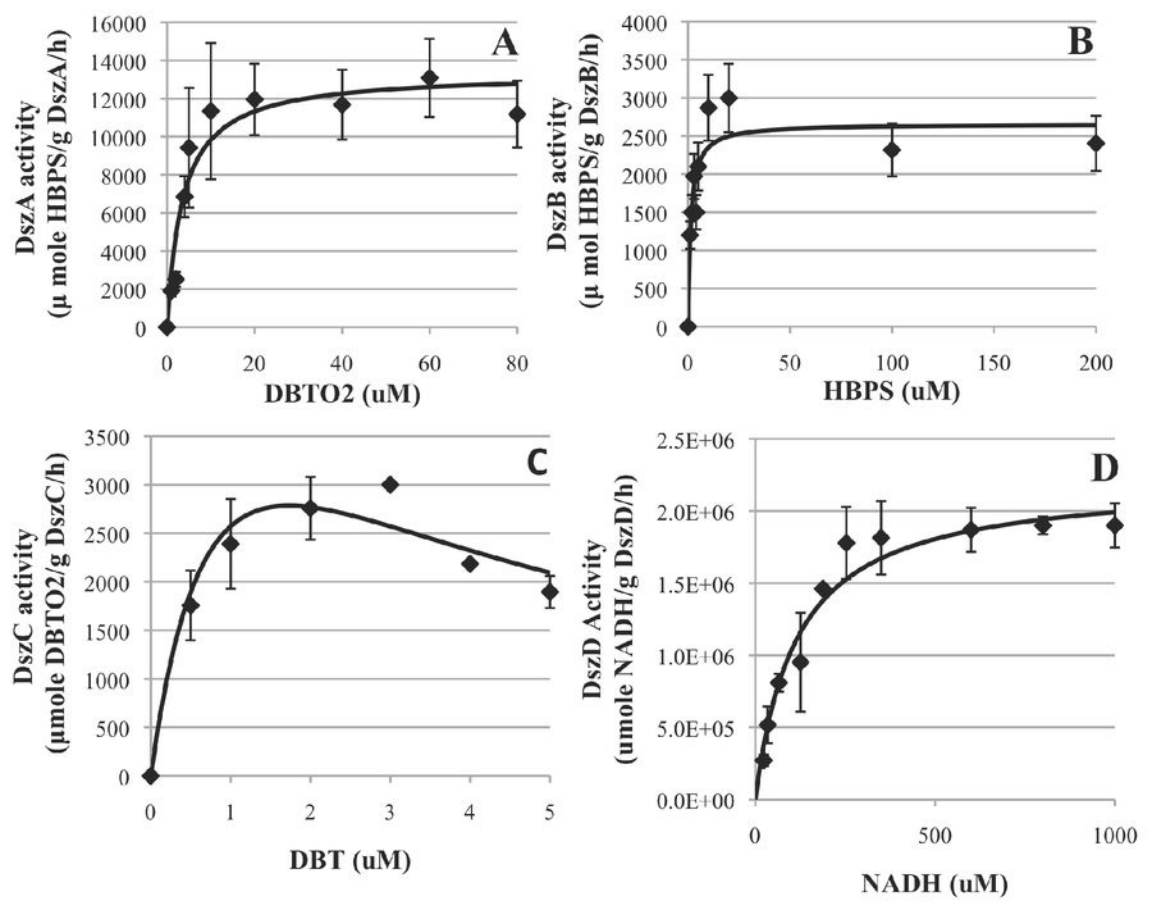
A
DszA activity
(µ mole HBPS/g DszA/h)
DBTO2 (uM)
B
DszB activity
(µ mol HBPS/g DszB/h)
HBPS (uM)
C
DszC activity
(µmole DBTO2/g DszC/h)
DBT (uM)
D
DszD Activity
(umole NADH/g DszD/h)
NADH (uM)

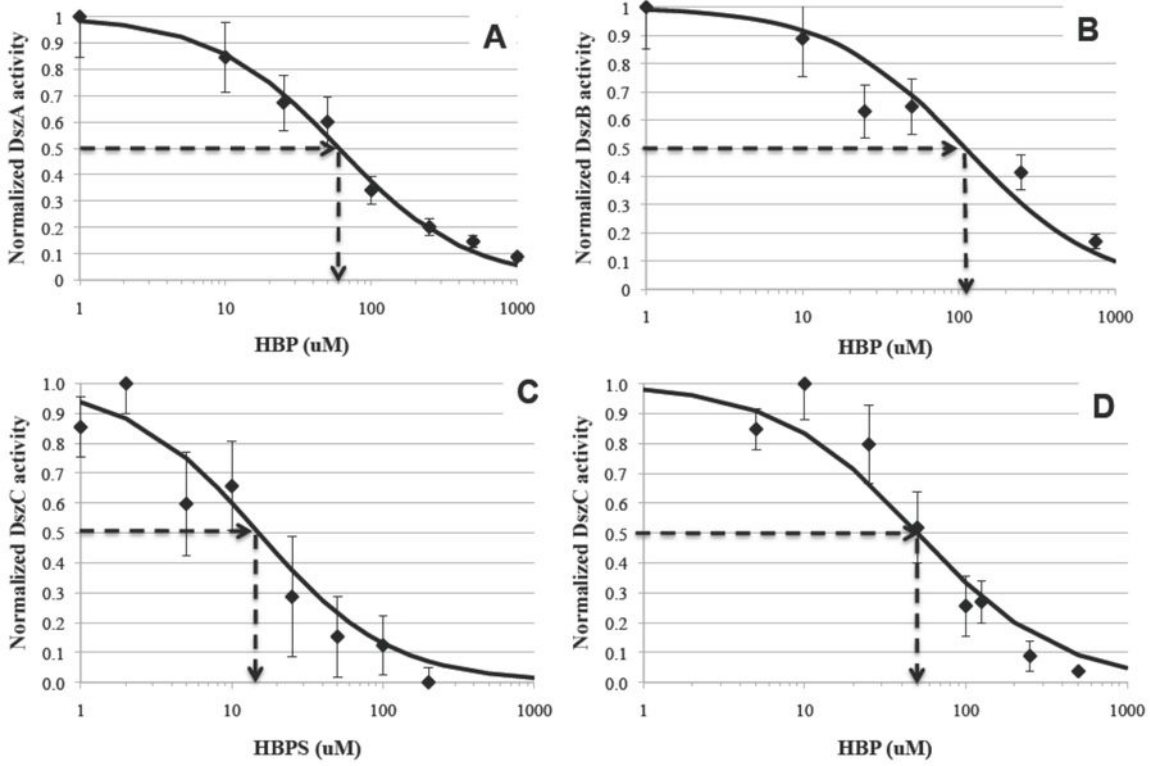
A
Normalized DszA activity
HBP (uM)
B
Normalized DszB activity
HBP (uM)
C
Normalized DszC activity
HBPS (uM)
D
Normalized DszC activity
HBP (uM)

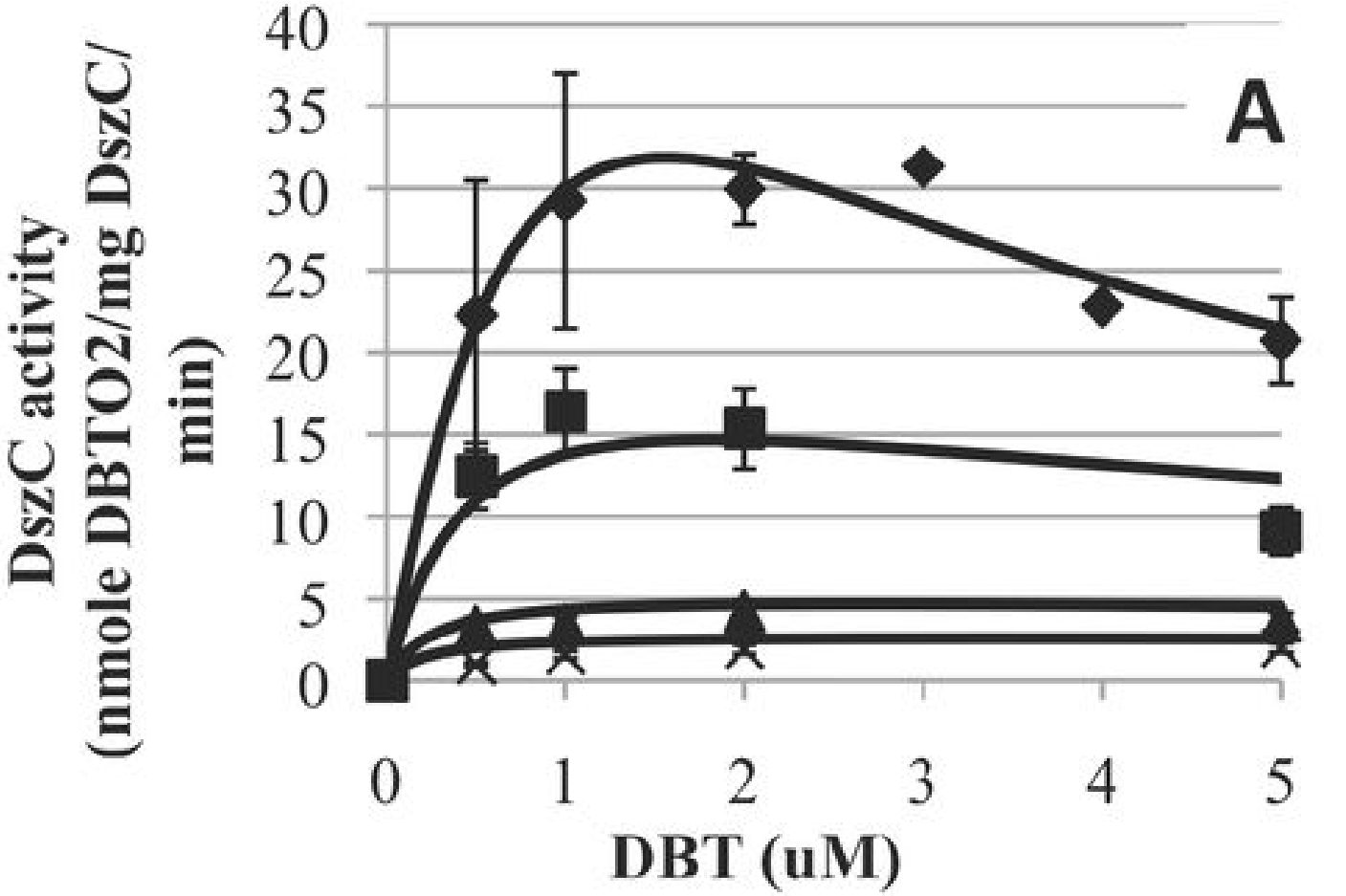
A
DszC activity (nmole DBTO2/mg DszC/ min)
40
35
30
25
20
15
10
5
0
0
1
2
3
4
5
DBT (uM)

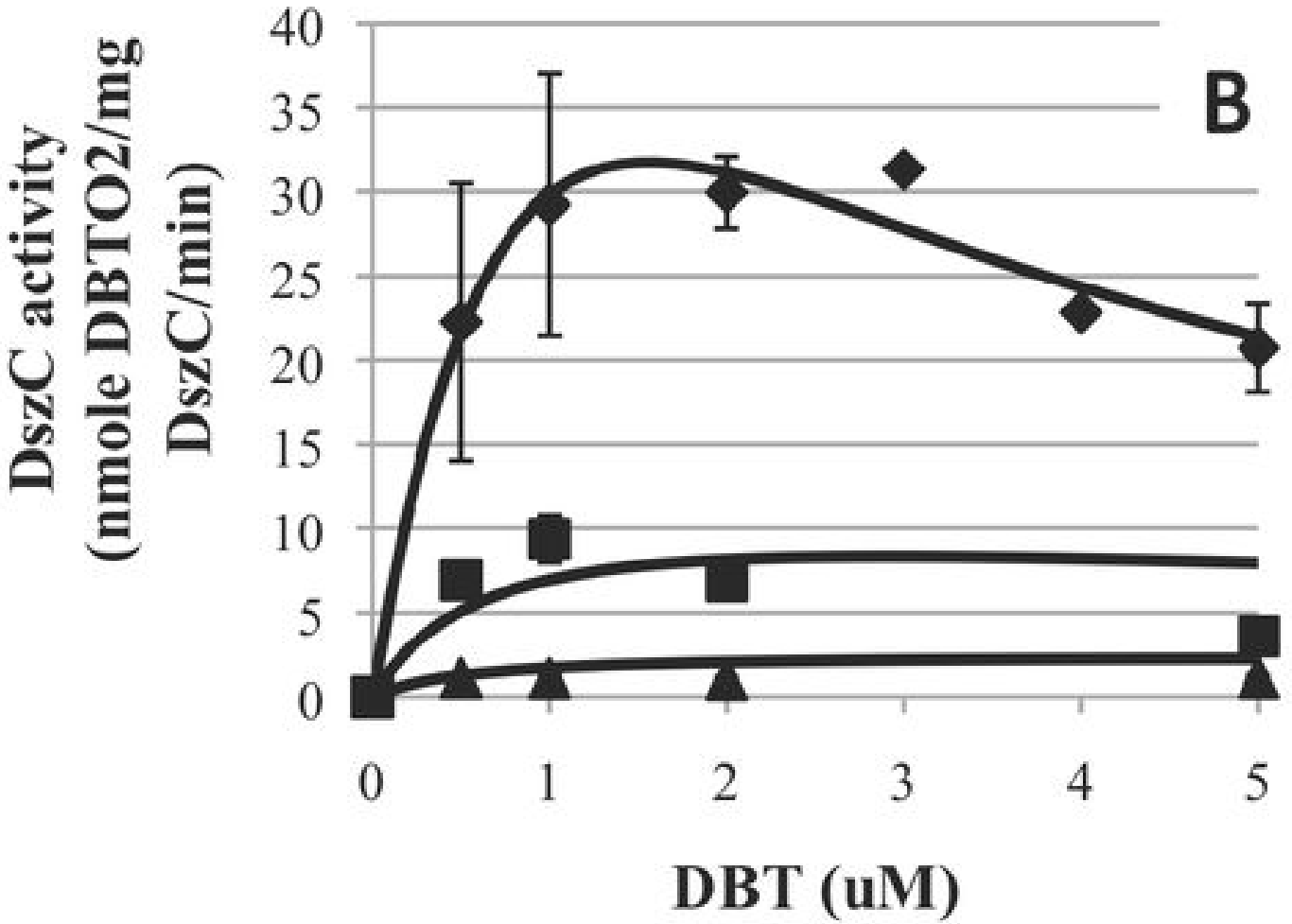
B
DszC activity (nmole DBTO2/mg DszC/min)
40
35
30
25
20
15
10
5
0
0
1
2
3
4
5
DBT (uM)

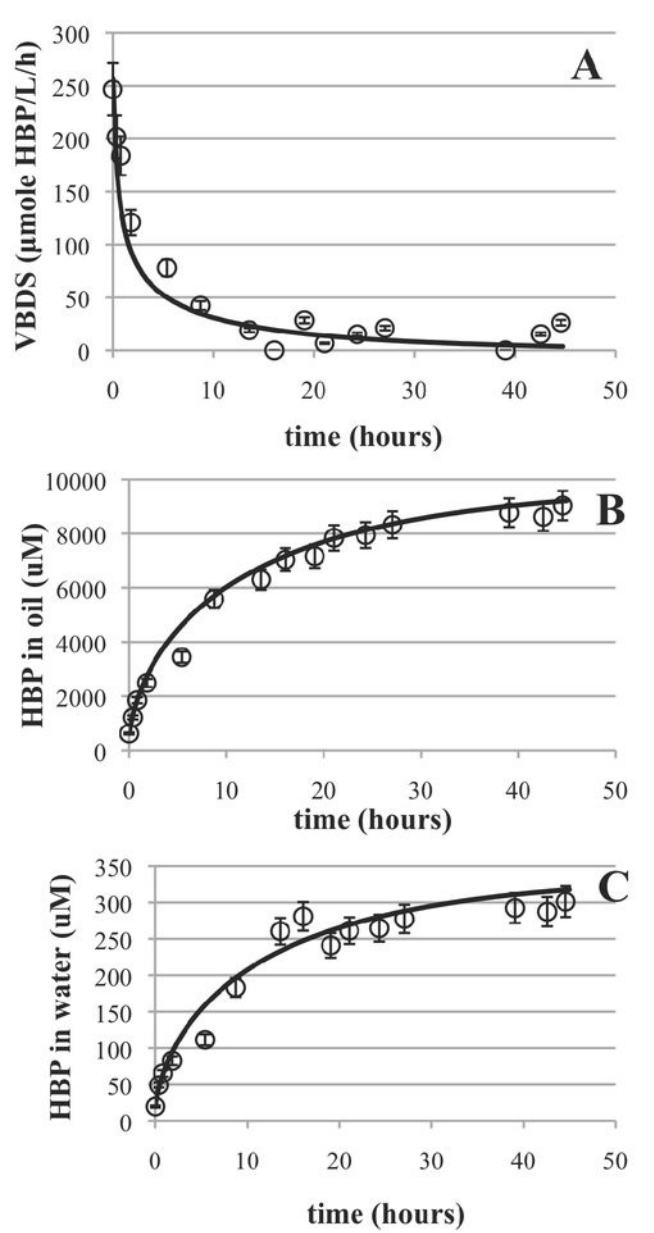
A
VBDS (µmole HBP/L/h)
300
250
200
150
100
50
0
0
10
20
30
40
50
time (hours)
B
HBP in oil (uM)
10000
8000
6000
4000
2000
0
0
10
20
30
40
50
time (hours)
C
HBP in water (uM)
350
300
250
200
150
100
50
0
0
10
20
30
40
50
time (hours)